SIMPLIFIED PREDICTIVE MODELS FOR CO₂ SEQUESTRATION PERFORMANCE ASSESSMENT

FINAL PROJECT REPORT

Reporting Period: October 1, 2012 through September 30, 2015

Principal Investigator: Dr. Srikanta Mishra
mishras@battelle.org 614-424-5712

Principal Authors: Srikanta Mishra, Priya Ravi Ganesh, Jared Schuetter,
Jincong He, Zhaoyang Jin and Louis J. Durlofsky

Submitting Organization:
Battelle Memorial Institute
505 King Avenue
Columbus, OH 43201
DUNS Number: 00 790 1598

Abstract

CO_2 sequestration in deep saline formations is increasingly being considered as a viable strategy for the mitigation of greenhouse gas emissions from anthropogenic sources. In this context, detailed numerical simulation based models are routinely used to understand key processes and parameters affecting pressure propagation and buoyant plume migration following CO_2 injection into the subsurface. As these models are data and computation intensive, the development of computationally-efficient alternatives to conventional numerical simulators has become an active area of research. Such simplified models can be valuable assets during preliminary CO_2 injection project screening, serve as a key element of probabilistic system assessment modeling tools, and assist regulators in quickly evaluating geological storage projects. We present three strategies for the development and validation of simplified modeling approaches for CO_2 sequestration in deep saline formations: (1) simplified physics-based modeling, (2) statistical-learning based modeling, and (3) reduced-order method based modeling.

In the first category, a set of full-physics compositional simulations is used to develop correlations for dimensionless injectivity as a function of the slope of the CO_2 fractional-flow curve, variance of layer permeability values, and the nature of vertical permeability arrangement. The same variables, along with a modified gravity number, can be used to develop a correlation for the total storage efficiency within the CO_2 plume footprint. Furthermore, the dimensionless average pressure buildup after the onset of boundary effects can be correlated to dimensionless time, CO_2 plume footprint, and storativity contrast between the reservoir and caprock.

In the second category, statistical "proxy models" are developed using the simulation domain described previously with two approaches: (a) classical Box-Behnken experimental design with a quadratic response surface, and (b) maximin Latin Hypercube sampling (LHS) based design with a multi-dimensional kriging metamodel fit. For roughly the same number of simulations, the LHS-based metamodel yields a more robust predictive model, as verified by a *k*-fold cross-validation approach (with data split into training and test sets) as well by validation with an independent dataset.

In the third category, a reduced-order modeling procedure is utilized that combines proper orthogonal decomposition (POD) for reducing problem dimensionality with trajectory-piecewise linearization (TPWL) in order to represent system response at new control settings from a limited number of training runs. Significant savings in computational time are observed with reasonable accuracy from the POD-TPWL reduced-order model for both vertical and horizontal well problems – which could be important in the context of history matching, uncertainty quantification and optimization problems.

The simplified physics and statistical learning based models are also validated using an uncertainty analysis framework. Reference cumulative distribution functions of key model outcomes (i.e., plume radius and reservoir pressure buildup) generated using a 97-run full-physics simulation are successfully validated against the CDF from 10,000 sample probabilistic simulations using the simplified models.

The main contribution of this research project is the development and validation of a portfolio of simplified modeling approaches that will enable rapid feasibility and risk assessment for CO_2 sequestration in deep saline formations.

Table of Contents

List of Tables

List of Figures

Page

Executive Summary

The objective of this research project is to develop and validate a portfolio of simplified modeling approaches for CO$_2$ sequestration in deep saline formations – based on simplified physics, statistical learning, and/or mathematical approximations – for predicting: (a) injection well and formation pressure buildup, (b) lateral and vertical CO$_2$ plume migration, and (c) brine displacement to overlying formations and the far-field. Such computationally-efficient alternatives to conventional numerical simulators can be valuable assets during preliminary CO$_2$ injection project screening, serve as a key element of probabilistic system assessment modeling tools, and assist regulators in quickly evaluating geological storage projects. The project team includes Battelle and Stanford University. Support for the project is provided by U.S. DOE National Energy Technology Laboratory and the Ohio Development Service Agency Office of Coal Development (ODSA).

Over the last decade, the development and demonstration of geologic sequestration technologies to mitigate greenhouse gas emissions has been an area of active research. Geologic sequestration of CO$_2$ in deep saline formations has been recognized for its immense potential for long-term storage of captured CO$_2$. To ensure safe and effective deployment of this technology, it is crucial for us to understand the nature of pressure and plume propagation as injected CO$_2$ displaces the native reservoir fluids. Detailed numerical simulation of such processes generally requires extensive reservoir characterization data and computational burden. In this context, validated simplified models can be valuable as they have minimal data and computational requirements in comparison. Simplified models that are based on the most relevant physical processes and validated against full-physics simulators are thus being sought after as efficient and useful alternatives for rapid screening and evaluation of CO$_2$ sequestration projects. The research carried out under this project utilizes three broad approaches: (a) simplified physics-based modeling, (b) statistical-learning based modeling, and (c) reduced-order method based modeling. Finally, an uncertainty and sensitivity analysis based validation framework is used to compare the results of full-physics and simplified models from probabilistic simulations.

In the simplified-physics based approach, only the most important physical processes are modeled to develop and validate simplified predictive models of CO$_2$ sequestration in deep saline formation. The system of interest is a single vertical well injecting supercritical CO$_2$ into a 2-D layered reservoir-caprock system with variable layer permeabilities. A set of well-designed full-physics compositional simulations is used to understand key processes and parameters affecting pressure propagation and buoyant plume migration. Based on these simulations, correlations have been developed for dimensionless injectivity as a function of the slope of CO$_2$-water fractional-flow curve, variance of layer permeability values, and the nature of vertical permeability arrangement. The same variables, along with a modified gravity number, can be used to develop a correlation for the total storage efficiency within the CO$_2$ plume footprint. Correlations are also developed to predict the average pressure buildup within the injection reservoir, as well as the pressure buildup within the caprock. These correlations are generally found to have good predictive ability.

In statistical-learning based modeling, two approaches are compared for building a statistical proxy model (metamodel) for CO$_2$ geologic sequestration from the results of full-physics compositional simulations. The first approach involves a classical Box-Behnken or Augmented Pairs experimental design with a

quadratic polynomial response surface. The second approach uses a space-filling maximin Latin Hypercube sampling (LHS) or maximum entropy design with the choice of five different meta-modeling techniques: quadratic polynomial, kriging with constant and quadratic trend terms, multivariate adaptive regression spline (MARS) and additivity and variance stabilization (AVAS). Simulations results for CO$_2$ injection into a reservoir-caprock system with 9 design variables (and 97 samples) were used to generate the data for developing the proxy models. The fitted models were validated with using an independent data set and a cross-validation approach for three different performance metrics: total storage efficiency, CO$_2$ plume radius and average reservoir pressure. The Box-Behnken–quadratic polynomial metamodel and the maximin LHS–kriging metamodel performed almost the same.

Reduced-order models provide a means for greatly accelerating the detailed simulations that will be required to manage CO$_2$ storage operations. This work investigates one such method, POD-TPWL, which has previously been shown to be effective in oil reservoir simulation problems. The method combines trajectory piecewise linearization (TPWL), in which the solution to a new (test) problem is represented through a linearization around the solution to a previously-simulated (training) problem, with proper orthogonal decomposition (POD), which enables solution states to be expressed in terms of a relatively small number of parameters. The application of POD-TPWL for CO$_2$-water systems is simulated using a compositional procedure. Stanford's Automatic Differentiation-based General Purpose Research Simulator (AD-GPRS) performs the full-order training simulations and provides the output (derivative matrices and system states) required by the POD-TPWL method. A new POD-TPWL capability introduced in this work is the use of horizontal injection wells that operate under rate (rather than bottom-hole pressure) control. Simulation results are presented for CO$_2$ injection into a synthetic aquifer and into a simplified model of the Mount Simon formation. Test cases involve the use of time-varying well controls that differ from those used in training runs. Results of reasonable accuracy are consistently achieved for relevant well quantities. Runtime speedups of around a factor of 370 relative to full-order AD-GPRS simulations are achieved, though the preprocessing needed for POD-TPWL model construction corresponds to the computational requirements for about 2.3 full-order simulation runs. A preliminary treatment for POD-TPWL modeling in which test cases differ from training runs in terms of geological parameters (rather than well controls) is also presented.

One of the intended applications of simplified models is for performance assessment calculations, where the analyses are typically carried out in a probabilistic framework to deal with model and parameter uncertainty. It is therefore important to ensure that the simplified models are also capable of reproducing the full spectrum of uncertainty and sensitivity analysis results from detailed numerical simulators. A 97-run LHS design with the full-physics model is used to generate the reference cumulative distribution function (CDF) of two key outcomes: plume radius and average pressure buildup in the reservoir. This is compared against CDFs from 10,000-run LHS designs with three different models: (a) response surface from a Box-Behnken design and quadratic metamodel, (b) response surface from a maximin LHS design and kriging metamodel, and (c) simplified physics based methodology. The statistical learning-based simplified models are found to provide a more robust representation of the reference CDF, particularly with respect to outliers.

1. Introduction

1.1 Project Objectives

The objective of this research project is to develop and validate a portfolio of simplified modeling approaches for CO$_2$ sequestration in deep saline formations – based on simplified physics, statistical learning, and/or mathematical approximations – for predicting: (a) injection well and formation pressure buildup, (b) lateral and vertical CO$_2$ plume migration, and (c) brine displacement to overlying formations and the far-field. Such computationally-efficient alternatives to conventional numerical simulators can be valuable assets during preliminary CO$_2$ injection project screening, serve as a key element of probabilistic system assessment modeling tools, and assist regulators in quickly evaluating geological storage projects. The project team includes Battelle and Stanford University. Support for the project is provided by U.S. DOE National Energy Technology Laboratory and the Ohio Development Service Agency Office of Coal Development (ODSA).

Over the last decade, the development and demonstration of geologic sequestration technologies to mitigate greenhouse gas emissions has been an area of active research. Geologic sequestration of CO$_2$ in deep saline formations has been recognized for its immense potential for long-term storage of captured CO$_2$. To ensure safe and effective deployment of this technology, it is crucial for us to understand the nature of pressure and plume propagation as injected CO$_2$ displaces the native reservoir fluids. Detailed numerical simulation of such processes generally requires extensive reservoir characterization data and computational burden. In this context, validated simplified models can be valuable as they have minimal data and computational requirements in comparison. Simplified models that are based on the most relevant physical processes and validated against full-physics simulators are thus being sought after as efficient and useful alternatives for rapid screening and evaluation of CO$_2$ sequestration projects.

The project is organized around four main technical tasks:

Task 2 – simplified physics-based modeling, where only the most relevant physical processes are modeled,

Task 3 – statistical-learning based modeling, where the simulator is replaced with a "response surface",

Task 4 – reduced-order method based modeling, where mathematical approximations reduce the computational burden.

Task 5 – uncertainty and sensitivity analysis based validation, where probabilistic simulations are used to compare the results of full-physics and simplified models.

1.2 Summary of Topical Reports

Results of research activities related to Tasks 2-4 have been described in detail in a series of topical reports (Ravi Ganesh and Mishra, 2014 [1]; Schuetter and Mishra, 2014 [2]; Jin et al, 2015 [3]). The abstracts of these reports are presented below.

Simplified physics-based modeling (Ravi Ganesh and Mishra, 2014): We present a simplified-physics based approach, where only the most important physical processes are modeled, to develop and validate simplified predictive models of CO_2 sequestration in deep saline formation. The system of interest is a single vertical well injecting supercritical CO_2 into a 2-D layered reservoir-caprock system with variable layer permeabilities. We use a set of well-designed full-physics compositional simulations to understand key processes and parameters affecting pressure propagation and buoyant plume migration. Based on these simulations, we have developed correlations for dimensionless injectivity as a function of the slope of fractional-flow curve, variance of layer permeability values, and the nature of vertical permeability arrangement. The same variables, along with a modified gravity number, can be used to develop a correlation for the total storage efficiency within the CO_2 plume footprint. Similar correlations are also developed to predict the average pressure within the injection reservoir, as well as the pressure buildup within the caprock.

Statistical-learning based modeling (Schuetter and Mishra, 2014): We compare two approaches for building a statistical proxy model (metamodel) for CO_2 geologic sequestration from the results of full-physics compositional simulations. The first approach involves a classical Box-Behnken or Augmented Pairs experimental design with a quadratic polynomial response surface. The second approach used a space-filling maximin Latin Hypercube sampling or maximum entropy design with the choice of five different meta-modeling techniques: quadratic polynomial, kriging with constant and quadratic trend terms, multivariate adaptive regression spline (MARS) and additivity and variance stabilization (AVAS). Simulations results for CO_2 injection into a reservoir-caprock system with 9 design variables (and 97 samples) were used to generate the data for developing the proxy models. The fitted models were validated with using an independent data set and a cross-validation approach for three different performance metrics: total storage efficiency, CO_2 plume radius and average reservoir pressure. The Box-Behnken–quadratic polynomial metamodel performed the best, followed closely by the maximin LHS–kriging metamodel.

Reduced-order method based modeling (Jin et al., 2015): Reduced-order models provide a means for greatly accelerating the detailed simulations that will be required to manage CO_2 storage operations. In this work, we investigate the use of one such method, POD-TPWL, which has previously been shown to be effective in oil reservoir simulation problems. This method combines trajectory piecewise linearization (TPWL), in which the solution to a new (test) problem is represented through a linearization around the solution to a previously-simulated (training) problem, with proper orthogonal decomposition (POD), which enables solution states to be expressed in terms of a relatively small number of parameters. We describe the application of POD-TPWL for CO_2-water systems simulated using a compositional procedure. Stanford's Automatic Differentiation-based General Purpose Research Simulator (AD-GPRS) performs the full-order training simulations and provides the output (derivative matrices and system states) required by the POD-TPWL method. A new POD-TPWL capability introduced in this work is the use of horizontal injection wells that operate under rate (rather than bottom-hole pressure) control. Simulation results are presented for CO_2 injection into a synthetic aquifer and into a simplified model of the Mount Simon formation. Test cases involve the use of time-varying well controls that differ from those used in training runs. Results of reasonable accuracy are consistently achieved for relevant well quantities. Runtime speedups of around a factor of 370 relative to full-order AD-GPRS simulations are achieved, though the preprocessing needed for POD-TPWL model construction corresponds to the computational requirements for about 2.3 full-order simulation runs. A preliminary treatment for POD-

TPWL modeling in which test cases differ from training runs in terms of geological parameters (rather than well controls) is also presented. Results in this case involve only small differences between training and test runs, though they do demonstrate that the approach is able to capture basic solution trends.

1.3   Organization of Report

The report is divided into two main parts. Chapter 2 provides a summary of the topical reports for Tasks 2-4 in the form of a paper that was prepared for presentation at the 2015 Annual Technical Conference and Exhibition of the Society of Petroleum Engineers (Mishra et al., 2015 [4]). Chapter 3 presents the results of Task 5, i.e., validation of simplified modeling approaches using uncertainty and sensitivity analysis. Finally, Chapter 4 presents conclusions from this study, and recommendations for future work. Also, excerpts from the Topical Reports (i.e., abstract, table of contents, list of tables, list of figures and executive summary) are included in the Appendix.

References

[1] Ravi Ganesh, P. and Mishra, S., 2014. Simplified Physics Based Predictive Models for CO$_2$ Sequestration Performance Assessment, Task 2 Topical Report. US Department of Energy, National Energy Technology Laboratory, Pittsburgh, PA, 158 pp.

[2] Schuetter, J. and Mishra, S., 2014. Statistical Learning Based Predictive Models for CO$_2$ Sequestration Performance Assessment, Task 3 Topical Report. US Department of Energy, National Energy Technology Laboratory, Pittsburgh, PA, 75 pp.

[3] Jin, L.-Z., J. He and L. Durlofsky, 2015. Reduced-Order Method Based Predictive Models for CO$_2$ Sequestration Performance Assessment, Task 4 Topical Report. US Department of Energy, National Energy Technology Laboratory, Pittsburgh, PA, 98 pp.

[4] Mishra, S., P. Ravi Ganesh, J. Schuetter, J. He, Z. Jin and L. Durlofsky, 2015. Developing and Validating Simplified Predictive Models for CO$_2$ Geologic Sequestration. SPE 175097, Proc., SPE Annual Technical Conference and Exhibition, Houston, TX, 28-30 September.

2. Developing and Validating Simplified Predictive Models of CO_2 Geologic Sequestration

2.1 Introduction

CO_2 injection into the sub-surface is emerging as a viable technology for reducing anthropogenic CO_2 emissions into the atmosphere [1]. Deep saline formations provide a particularly attractive target for this purpose, with potential storage capacity in such systems in North America estimated to be of the order of 3400 billion tons of CO_2, or the equivalent of emissions from hundreds of years [2]. Over the last decade, the development and demonstration of geologic sequestration technologies to mitigate greenhouse gas emissions has been a field of active study. The U.S. Department of Energy's (DOE's) Carbon Storage Program has provided the primary impetus for R&D activities in the U.S. to develop and advance technologies that will significantly improve the efficacy of the geologic carbon storage technology, reduce the cost of implementation, and be ready for widespread commercial deployment between 2020 and 2030.

When large amounts of CO_2 are sequestered underground, excess pressure buildup in the storage formations and cap rock is an associated risk in terms of endangering integrity of underground formation and wellbores, along with the risk of potential plume movement beyond the injected domain. Multiple technologies related to the evaluation of capacity and injectivity, monitoring of CO_2 plume movement, and risk assessment are needed to ensure safe and effective deployment of geologic storage. One key technology in this regard is the simulation of CO_2 injection and migration over very large areas and over long periods of time [3]. Detailed numerical models of CO_2 geological storage are, however, data and computation intensive. In this context, validated simplified analytical or semi-analytical modeling tools can be valuable assets in preliminary CO_2 injection project screening and implementation phases [4]. Such tools have minimal data and computational requirements compared to detailed-physics numerical simulators. Simplified models are therefore being sought after as alternatives for rapid feasibility and risk assessment of CO_2 sequestration projects [5].

The primary motivation for this study is to provide simplified modeling tools that will enable rapid feasibility and risk assessment of CO_2 sequestration projects in deep saline formations. These tools will: (a) provide project developers with quick and simple tools to screen sites and estimate monitoring needs, (b) provide regulators with tools to evaluate geological storage projects quickly without running full-scale detailed numerical simulations, (c) enable integrated system risk assessments to be carried out with robust, yet simple to implement, reservoir performance models, and (d) allow modelers to efficiently analyze the impact of variable CO_2 injection rates on plume migration and trapping for optimal well placement and rate allocation.

In this chapter, three strategies are described for the development and validation of simplified modeling approaches for CO_2 sequestration in deep saline formations: (1) simplified physics-based modeling, where only the most relevant physical processes are modeled, (2) statistical-learning based modeling, where the simulator is replaced with a "response surface", and (3) reduced-order method based modeling, where mathematical approximations reduce the computational burden.

The chapter is organized as follows. There are three main sections dealing with each of three strategies noted earlier. For each section, we provide a summary of the relevant literature, discuss the full-physics model that forms the basis for deriving the reduced-order models, and describe the methodology for simplified model formulation and validation. The chapter concludes with a discussion of the practical aspects for each modeling strategy and concluding remarks based on the study.

2.2 Simplified Physics Based Models

2.2.1 Background

Simplified models based on first principles can be extremely useful for rapid integrated system assessment of CO_2 sequestration projects. One common modeling approach builds upon a Buckley-Leverett type radial displacement formulation first presented for gas storage in aquifers [6], and subsequently adapted for the problem of CO_2 plume migration in deep saline aquifers [7, 8]. Others have developed corresponding expressions for injection well pressure buildup using various assumptions regarding the mobility of the two-phase region [9-11].

A second approach uses an elegant sharp interface approximation to front propagation that leads to closed-form expressions for plume radius [12, 13] and pressure propagation [14, 15]. As is the case with the Buckley-Leverett type models discussed earlier, this approach also assumes that the reservoir is homogeneous in both radial and vertical directions, bounded above and below by impermeable layers, and is infinite-acting in the radial direction.

Ref. [16] presented simple expressions for computing pressure buildup in reservoirs that were semi-confined (i.e., with permeable over and/or underlying layers) and closed (i.e., with finite lateral boundaries). Their solution is strictly valid for single-phase flow conditions, although they show reasonable agreement with two-phase simulations if the injected volumes are balanced. Similar relationships based on single-phase pseudo-steady state flow equations have also been presented [17].

Based on this literature review, we conclude that there is need for simplified models that account for pressure buildup and CO_2 plume migration in saline formations while taking into account two-phase flow conditions, vertical variations in permeability (which can affect plume stratification), semi-confined conditions (presence of a cap rock) and finite lateral extent (well injecting into a closed volume).

2.2.2 Modeling and Analysis Methodology

The computational model consists of a single vertical well radially injecting supercritical CO_2 in the middle of a 2D layered reservoir overlain by a cap rock. We add an overlying cap rock and vertically layered heterogeneity to previously considered simplified model geometries, thus introducing buoyancy and heterogeneity effects on plume migration. Our approach is based on a combination of first-principles and inspectional analysis from detailed numerical experiments using following workflow:

- Well-defined compositional simulations of CO_2 injection into a semi-confined cylindrical saline aquifer system are carried out for a broad range of reservoir and cap rock properties.

- Data from this sensitivity analysis exercise are used to develop insights into the relationship between the performance metrics of interest and fundamental reservoir/ cap rock properties. Inspectional analysis yields dimensionless groups for correlating the data.

- Regression analysis is used to represent dimensionless pressure buildup and total storage efficiency (defined below) as a function of the underlying independent variable groups identified from sensitivity analysis.

- The resulting predictive relationships are tested to validate the predictive models using "blind" runs with simulations not part of the "training set" (i.e., not used in the model formulation).

2.2.3 Model Description

The basic model is that of a single-well injecting supercritical CO_2 into a bounded 2D radial-cylindrical aquifer initially filled with brine. The model domain consists of a porous and permeable heterogeneous reservoir, overlain by a low-permeability cap rock. The top of the cap rock, the bottom of the reservoir and the lateral boundary are all assumed to be no-flow boundaries. Fig. 2-1 illustrates the system of interest and the grid defined. The simulations are executed in the numerical simulator GEM® developed by the Computer Modeling Group (CMG). The following simulation elements are considered for our system:

- A semi-confining system similar to the Mt Simon sandstone (reservoir) – Eau Claire shale (cap rock) configuration in the Illinois basic [20]
- Reservoir and cap rock thickness (and variants) similar to that used for the Arches project [18,19]
- Reservoir permeability and porosity (and variants) similar to that used for the Arches project [18,19]
- Cap rock permeability and air entry pressure from the Illinois basin project [20]
- Permeability variation and anisotropy ratio assumed over a realistic range
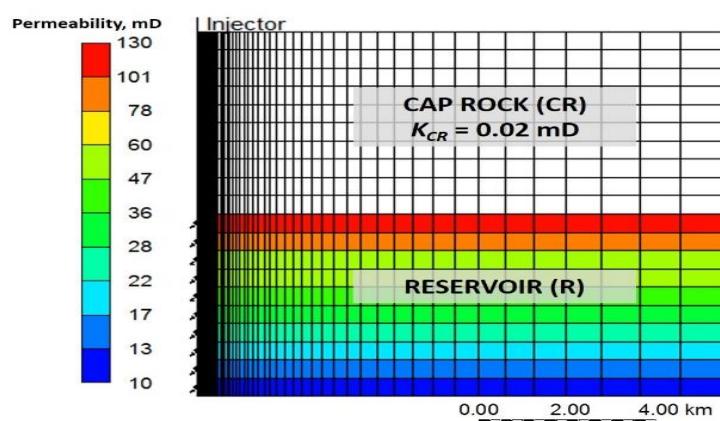
Fig. 2-1. Model geometry and gridding for the system of interest.

(A) Simulation Scenarios

Simulations are run to observe CO_2 displacement characteristics for an injection period of 30 years in a closed system – as would be the case in a network of injection wells. The independent variables of interest are thickness and porosity of reservoir and cap rock, reservoir permeability heterogeneity, permeability and capillary pressure of the cap rock, and CO_2 injection rate. Reservoir heterogeneity is varied by controlling the mean reservoir permeability, permeability anisotropy ratio (ratio of vertical to horizontal permeability) in the reservoir, spatial arrangement of the heterogeneous reservoir permeability layers, and relative permeability curves for the reservoir. We investigate the sensitivity of system behavior for high and low variants from a reference case for each of these variables and seek to quantify their effect on the dimensionless pressure buildup in the reservoir.

There are 10 independent variables identified in Table 2-1. A set of one-off simulations are carried out to develop a library of results from which insights related to the development of simplified-physics based model will be extracted. For each of these simulations, all other independent variables are kept fixed at their reference values. This simulation matrix is run with each of the three different relative permeability models described next.

Relative permeability curves for the reservoir are taken from [21]. Relative permeability curves are assumed to be the same for the caprock in all cases. These curves are shown in Fig. 2-2 (a). As far as variations from the reference case, the gas relative permeability curve for the reservoir is assumed to be linear for one of the variants (case A), whereas the other variant (case B) lies somewhere in between. The three separate curves provide a range of permeability characteristics for the reservoir model. Fig. 2-2 (b) shows the characterization of these relative permeability models using the slopes of the tangents to their gas fractional flow curves, i.e. df_g/dS_g. A total of 60 simulations cover all one-off parameter variations.

Table 2-1. Summary of test cases explored with parameter values for the reference case and the two variants.

	Parameter	Description	Units	Reference Value	Low Value	High Value	Comments
1	h_R	Thickness of reservoir	m	150	50	250	
2	h_{CR}	Thickness of caprock	m	150	100	200	
3	k_R	Average horizontal permeability of reservoir	mD	46	12	220	
	V_{DP}	Dykstra-Parsons coefficient	–	0.55	0.35	0.75	Correlated with k_R

| 4	k_{CR}	Average horizontal permeability of caprock	mD	0.02	0.002	0.2	
5	k_V/k_H	Anisotropy ratio	–	0.1	0.01	1	
6	q	CO₂ injection rate	MMT/yr	0.83	0.33	1.33	
			bbl/day	~17074	~7238	~25855	Averages from the reference case
	L	Outer radius of reservoir	m	10000	5000	7000	Correlated with q
7	ϕ_R	Porosity of reservoir	–	0.12	0.08	0.18	
8	ϕ_{CR}	Porosity of caprock	–	0.07	0.05	0.1	
9	$P_{C,CR}$	Capillary pressure model of caprock	–	reference	decreased Pc by ×3	increased Pc by ×3	
10	I_k	Permeability layering	–	random		increasing from bottom	
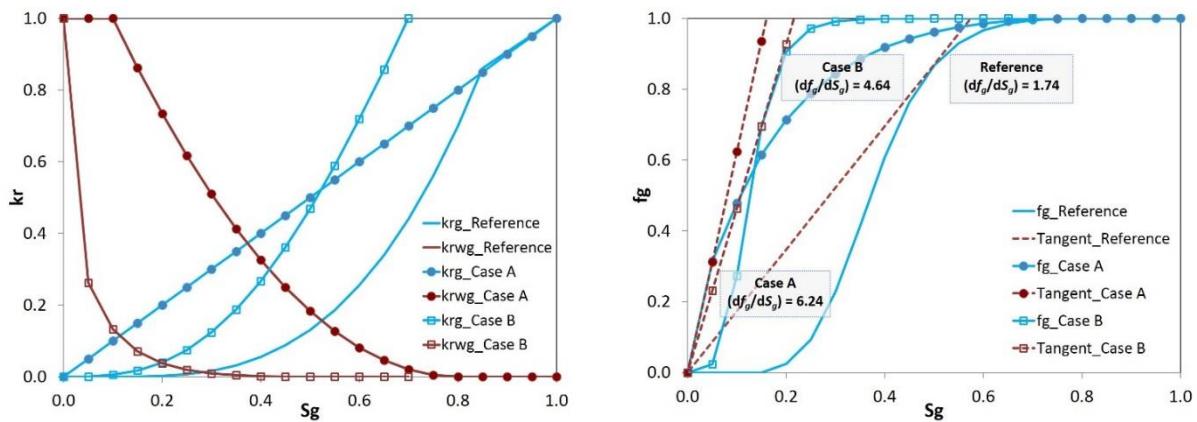
Fig. 2-2. (a) Relative permeability model variations, with different gas-water relative permeability curves (left panel); (b) Fractional flow curves for the three relative permeability models characterized in terms of their slopes (right panel).

(B) Predicting dimensionless pressure buildup and injectivity

Our objective here is to develop a simplified model for dimensionless pressure buildup at the injection well as a function of key reservoir and fluid properties. This model can be used to predict the injectivity (i.e., ratio of injection rate to pressure buildup) in similar layered aquifer systems, given their respective system parameters. We describe the process of formulating and validating the predictive model for CO_2 injectivity below.

From our sensitivity analysis simulations, we consistently observe that CO_2 begins displacing brine in the reservoir with an initial pressure jump followed by a transient period of quasi-steady injection well pressure. Once the pressure front reaches the lateral boundary of our system, further CO_2 injection causes additional pressure buildup in the reservoir as expected. The pressure jump at the well can be converted into a dimensionless quantity (P_D) using Eq. 2-1.

$$P_D = \frac{2\pi k_R h_R}{q\mu_w} \Delta P_{jump}$$

(2-1)

where k_R is reservoir permeability, h_R is reservoir thickness, q is volumetric injection rate, μ_w is brine viscosity, and ΔP_{jump} is the observed value of the pressure jump.

Based on inspectional analysis, we find that the dimensionless pressure buildup can be characterized as a function of the following variable groups:

- Relative permeability model characterized by the slope of the tangent to the CO_2 fractional flow curve, df_g/dS_g
- Dykstra-Parsons coefficient, defined as

$$V_{DP} = \frac{(k_{50} - k_{84.1})}{k_{50}}$$

where k_{50} is median (i.e., 50th percentile) reservoir permeability, and $k_{84.1}$ is the reservoir permeability at the median + one standard deviation (i.e., 84.1th percentile), assuming a log-normal distribution.

Fig. 2-3 shows a plot of the dimensionless pressure jump, P_D, versus the slope of the fractional flow curve, df_g/dS_g, which characterizes the relative permeability relationship. From the minimal scatter in the data, we conclude that the relative permeability model has a strong impact on P_D and hence injectivity, while permeability heterogeneity as characterized by V_{DP} has only a second-order effect.
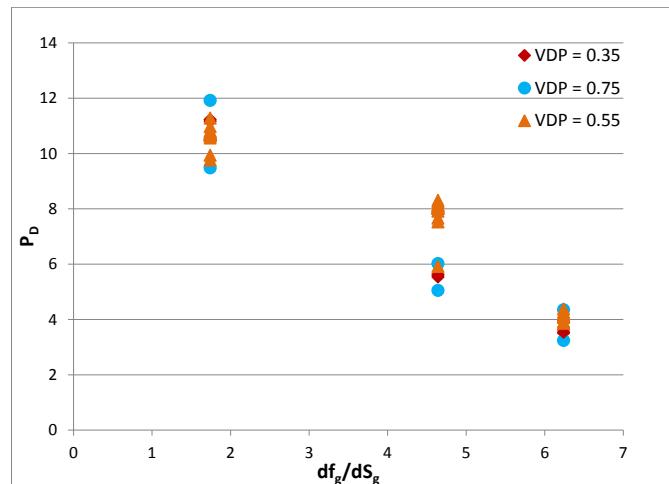
Fig. 2-3. Scatter plot of PD values for varying dfg/dSg and VDP.

The simulated data in Fig. 2-3 were fit to a multivariate quadratic regression model with interaction terms to yield the following relationship for P_D:

$$P_D = 10.3 + 0.59 \frac{df_g}{dS_g} + 3.41 V_{DP} + 1.23 \frac{df_g}{dS_g} V_{DP} - 0.342 \left(\frac{df_g}{dS_g} \right)^2 - 8.89 \left(V_{DP} \right)^2$$

(2-2)

Fig. 2-4 shows a comparison between the simulated values of P_D and those predicted with Eq. (2-2), indicating very good agreement. The coefficient of determination for this fit is $R^2 = 0.93$.

Injectivity index ($q/\Delta P_{jump}$) of the well is calculated from the dimensionless pressure buildup using Eq. 2-1. Fig. 2-5 compares the predicted injectivity indexes from our model with those calculated directly from the simulation dataset. The general equivalence between the model predictions and the simulations for the injectivity thus demonstrates the validity of our model.
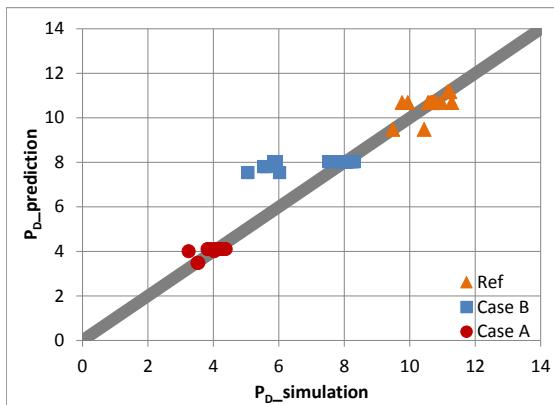

Fig. 2-4. Comparison plot between regression model Predictions and simulator output values for P_D.
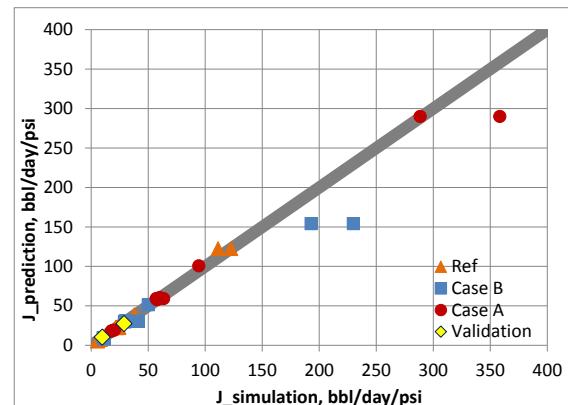

Fig. 2-5. Comparison plot between regression model predictions and simulator output values for $q/\Delta P$.

The simplified predictive model obtained for dimensionless pressure buildup (and hence for CO_2 injectivity) is also validated successfully for its robustness with two 'blind' simulation cases that were not part of the regression analysis, shown as yellow diamonds in Fig. 2-5. We find that the injectivity index predicted by our model for the first validation case is 10.5 bbl/day/psi compared to the simulation result of 9.6 bbl/day/psi. For the second validation case, the injectivity index predicted by our model is 27.5 bbl/day/psi compared to the simulation result of 28.7 bbl/day/psi. Thus, our simplified model (Eq. 2-2), together with Eq. 2-1, can be used to determine the CO_2 injection rate for a given target pressure differential, or alternatively, the pressure differential that would result from injecting CO_2 at a target rate.

2.2.4 Predicting average pressure buildup

For single-phase flow in closed systems, the dimensionless form of average reservoir pressure buildup can be written as [22]:

$$P_D = 2\pi t_{DA} = \frac{kh(\bar{P}-P_i)}{qB\mu} \; ; \; t_{DA} = \frac{kt}{\emptyset\mu c_t A} \quad (2\text{-}3)$$

where P_D is dimensionless pressure and t_{DA} is dimensionless time based on the drainage area, A. First, using simulated CO_2-brine displacement data with no-flow upper and lower boundaries (i.e., for a confined system), we investigate how this relationship changes for each of the three different relative permeability models shown in Fig. 2-2. In each of these cases, we notice a linear relationship between P_D and t_{DA}, as would be expected in the case of single-phase flow. However, the slope is always found to be lower than the single-phase value of (2π), which can be attributed to the effects of two-phase flow and the variability in the relative permeability models. The factor that quantifies the deviation from (2π), denoted by 'f', is postulated to be a function of the effectiveness of two-phase flow in the reservoir. This is dependent on the relative permeability model as well as the two-phase displacement dynamics. A proxy for the effectiveness of this displacement is the plume extent. Hence we determine 'f' to be directly related to the ratio of the system size to the plume extent, as shown in Fig. 2-6.
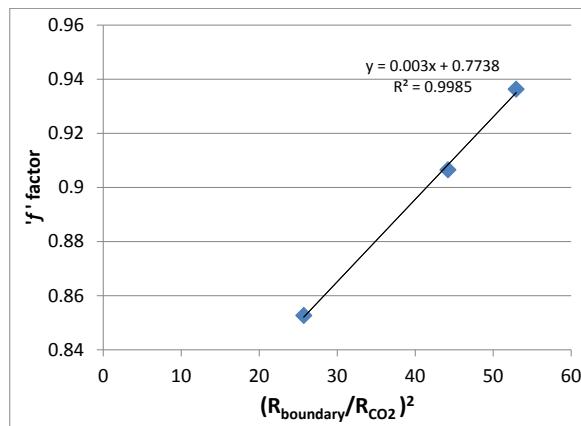
**Fig. 2-6. The 'f' factor for closed reservoirs is correlated to the square of the ratio of the reservoir radius to the plume radius at the end of injection.**

The next step is to determine the effect of reservoir and cap rock properties on 'f'' in semi-confined systems. We can express this in terms of a modified form of Eq. (2-3), viz.

$$P_D = f_{SC} \cdot f \cdot 2\pi t_{DA} \qquad (2\text{-}4)$$

We expect that 'f_{SC}' changes with varying storage capacity of the rock for each relative permeability model. All the simulation cases for all three relative permeability models have been analyzed to study the effect of rock properties on the slope factor. The 'f_{SC}' factor was found to be essentially equivalent to the storativity ratio, i.e., ratio of the porosity-thickness of the reservoir to the total porosity-thickness of the system:

$$f_{SC} = \frac{\emptyset_R h_R}{\emptyset_R h_R + \emptyset_{CR} h_{CR}} \qquad (2\text{-}5)$$

We summarize the results for each relative permeability model in Fig. 2-7, which compares f_{SC} calculated from the simulation results to that predicted by Eq. 2-5, thus indicating the robustness of this simple analytical proxy.
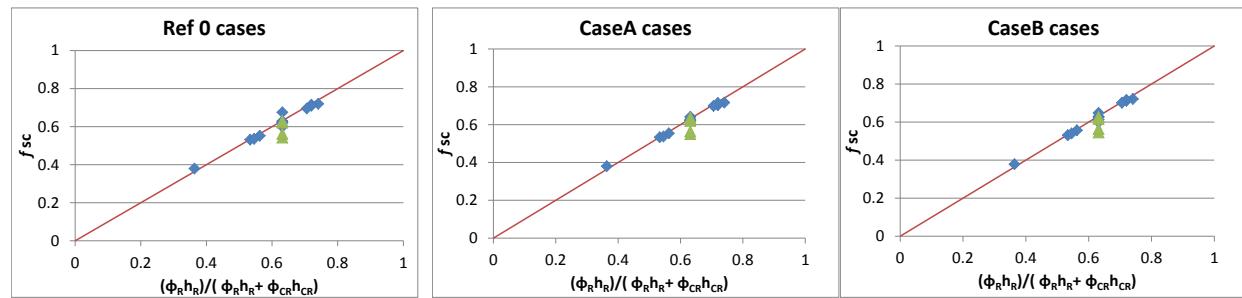

Fig. 2-7. Plot illustrating equivalence of fSC and ratio of porosity-thickness of the reservoir to the total porosity-thickness of the system (cap rock + reservoir) for all three relative permeability models.

2.2.5   Predicting total storage efficiency and plume radius

Our objective here is to develop a simplified model to estimate the outer extent of the CO₂-brine interface at the end of CO₂ injection in the reservoir. It is useful to define a few concepts using a schematic of the plume as shown in Fig. 2-8. Within the plume footprint, the fraction of the total pore volume in the reservoir contacted by CO₂ is given by the volumetric sweep efficiency (E_v). This is the ratio of the volume swept (contacted) by CO₂ to the total volume within the footprint of the CO₂ plume. Within this swept volume, the efficiency of displacement of the native brine by the CO₂ is given by the displacement efficiency. Because the initial gas saturation in the reservoir is zero, the average CO₂ saturation behind the front, $S_{g,av}$, gives this displacement efficiency [24]. The total storage efficiency E_s, defined as the product of E_v and $S_{g,av}$, thus signifies the efficiency of CO₂-brine displacement process or the ability to effectively sequester CO₂ in that reservoir. The lesser the value of total storage efficiency, the farther the areal footprint of the plume would be from the injection well.
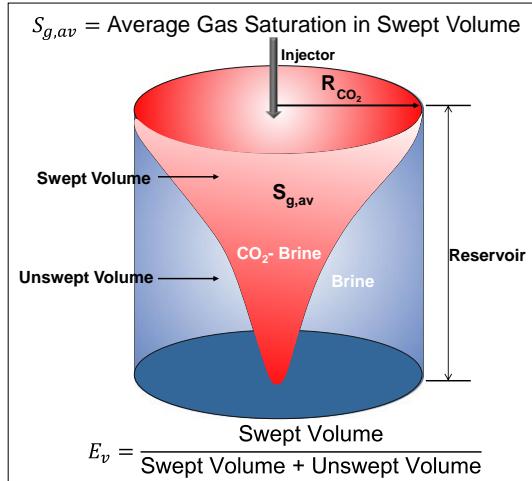
Fig. 2-8. System schematic showing graphical definition of plume
extent, volumetric sweep and displacement efficiency.

E_S is related to the maximum radial extent of the CO_2 plume at the end of injection, R, as given in Eq. 6
below:

$$R^2 = \frac{Q}{\pi \phi_R h_R S_{g,av} E_v} = \frac{Q}{\pi \phi_R h_R E_S} \quad (2\text{-}6)$$

R can be calculated for a given injection volume and reservoir storativity (porosity-thickness product), if
we can compute E_S as a function of fundamental inputs using Eq. 6. For our heterogeneous system, we
can draw comparison of E_S terms with the volumetric sweep and displacement efficiencies from other
simplified models in literature. The classic Buckley-Leverett theory gives the average gas saturation
($S_{g,av}$) to be the reciprocal of the shock velocity, i.e., slope to the tangent of the gas fractional flow curve,
df_g/dS_g [6]. In ideal homogeneous storage formations, perfect sweep efficiency ($E_V = 1$) is achieved such
as that considered in [7-8].

Based on first principles and the sensitivity analysis exercise described earlier, we characterize total
storage efficiency as a function of the following variable groups:

- Gravity number is a ratio of gravity and viscous effects. We define the dimensionless gravity
  number while accounting for the reservoir permeability anisotropy as:

$$N_g = \frac{(\Delta \rho g h_R) k_R h_R (\frac{h_R}{L})}{q \mu_g \left(\frac{k_V}{k_H}\right)} \quad (2\text{-}7)$$

The definition for gravity number in surveyed literature varies from source to source [23]. However the
fundamental behavior of this number remains the same through all definitions as to when the gravity
effects are more pronounced compared to the viscous flow effects (such as in thicker reservoirs) and vice-
versa.

- The heterogeneity of the reservoir, in terms of its spatial variation in permeability, is
  characterized by the Dykstra-Parsons coefficient, V_{DP}

- The heterogeneity of the reservoir can also be characterized in terms of the Lorenz coefficient which is related to the Dykstra-Parsons coefficient. It is defined as [24]:

$$L_C = 2 \left\{ \int_0^1 F_n dC_n - \frac{1}{2} \right\} \quad (2\text{-}8)$$

where F_n = cumulative flow capacity = $\frac{\sum_{i=1}^n k_{Ri} h_{Ri}}{\sum_{i=1}^N k_{Ri} h_{Ri}}$;

and C_n = cumulative storage capacity = $\frac{\sum_{i=1}^n \phi_{Ri} h_{Ri}}{\sum_{i=1}^N \phi_{Ri} h_{Ri}}$

The Lorenz coefficient also ranges from 0 to 1 with L_C being null for homogeneous reservoirs and closer to one for extremely heterogeneous ones. We calculate the Lorenz coefficient by honoring the permeability layering from the bottom-most to the top-most layer of the reservoir.

- Relative permeability model characterized by the slope of the tangent to CO$_2$ fractional flow curve, df_g/dS_g.

Fig. 2-9 shows E_S plotted as a function of all four independent variables defined above. As in waterflooding, we see the dependence of the total efficiency on relative permeability, i.e., higher df_g/dS_g values tend to have lesser scatter. The effect of reservoir heterogeneity is captured from the dependency of E_S on both the Dykstra-Parsons coefficient and the Lorenz coefficient. Buoyant CO$_2$ displacing brine is also affected by gravity segregation which is shown from Fig. 2-9(c).
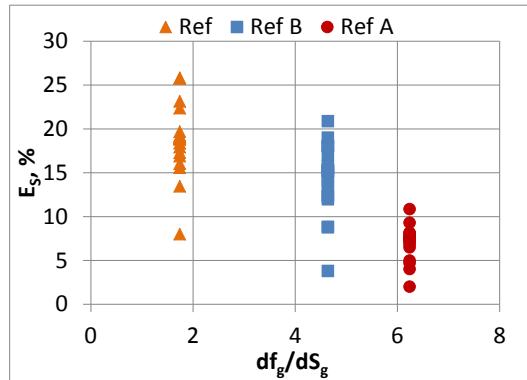

(a)
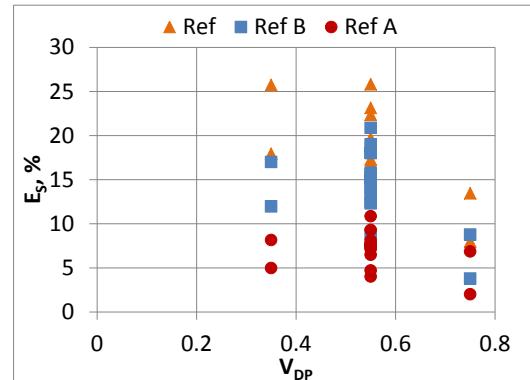
(b)
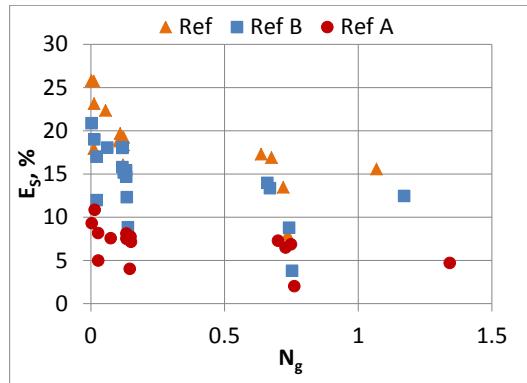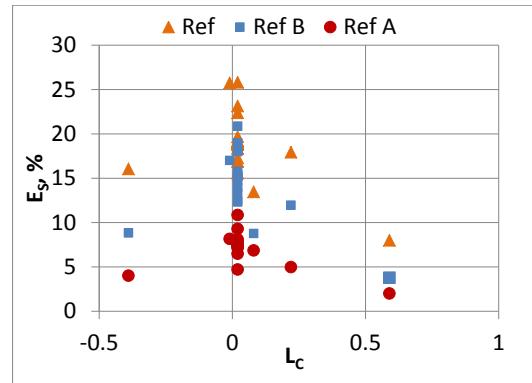
(c)   (d)

Fig. 2-9. Scatter plots of E_S values as a function of all four independent variables: (a) df_g/dS_g, (b) V_{DP}, (c) N_g, and (d) L_C.

The simulated data in Fig. 2-9 were fit to a multivariate quadratic regression model with interaction terms to yield the following relationship for E_S (in percent):

$$E_S = 30.7 + 0.435\frac{df_g}{dS_g} + 29.24L_C - 22.02V_{DP} - 11.2N_g + 4.59\frac{df_g}{dS_g}V_{DP}$$
$$- 25.21L_CV_{DP} - 0.692\left(\frac{df_g}{dS_g}\right)^2 + 6.11(N_g)^2$$

(2-9)

Fig. 2-10 shows the agreement between simulated and predicted values of E_S using our model, indicating very good agreement. The predicted total storage efficiency from Eq. 2-9 can be used to calculate the CO₂ plume extent for a given amount of CO₂ injected into the reservoir. Fig. 2-11 compares the predicted CO₂ plume extents (using predicted E_S in Eq. 2-6) for our simulations with the plume extents resulting from the respective simulations.
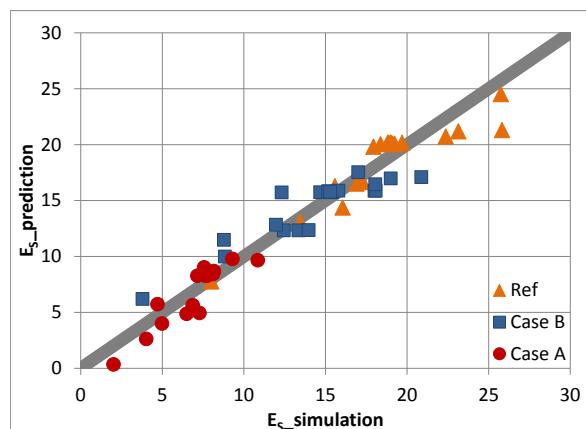

Fig. 2-10. Comparison plot between regression model predictions and simulator output values for E_S.
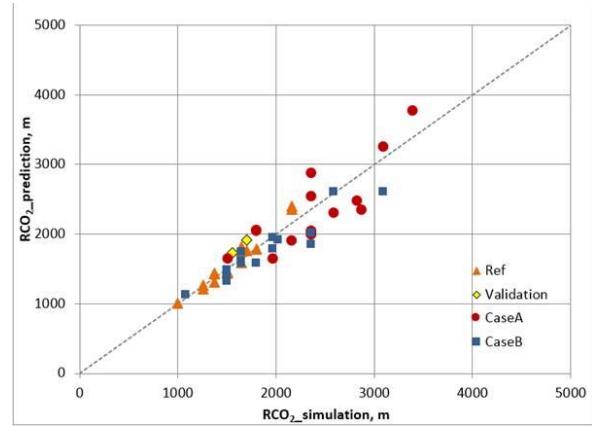

Fig. 2-11. Comparison plot between regression model predictions and simulator output values for R_{CO2}.

The simplified predictive model obtained for total storage efficiency and hence plume radius, is also validated for its robustness with two 'blind' simulation cases (shown as yellow diamonds in Fig. 2-11) that were not part of the regression analysis. We find that the plume radius predicted by our model for the first validation case is 1648 m compared to the simulation result of 1557 m. For the second validation case, the plume radius predicted by our model is 1794 m compared to the simulation result of 1670 m. Thus, our simplified model (equation 9) can be used to reasonably predict the total storage efficiency and hence determine the ultimate plume extent at the end of CO_2 injection from Eq. 2-6.

2.3 Statistical Learning Based Models

2.3.1 Background

The routine use of full-physics models for such tasks as uncertainty quantification, optimization and sensitivity analysis is often hindered by the computational burden of running repetitive simulations. Statistical-learning based modeling, also called proxy modeling, metamodeling or response surface modeling, is one common strategy for ameliorating this situation [25]. In this approach, an affordable sample of input settings is chosen, and the full physics model is run at those settings to obtain responses of interest. A proxy model or response surface is then fit to these data using statistical techniques. The proxy model is a functional approximation of the full-physics model for a given set of input values, albeit at a fraction of the computational cost of the full model. When the response in the full-physics model is well behaved and does not change erratically with respect to the input settings, proxy models can be quite accurate. When the response is less well behaved, the approximation could be poorer, at least in certain parts of the input space. However, even in these cases the proxy model can be useful for discovering the general parts of the input space that produce the most desirable response, at which time a more detailed study could be performed with the full physics model using only a small set of runs.

In the reservoir modeling literature, metamodels are often used as proxies for the underlying simulation models, especially for optimization and uncertainty quantification studies. Several studies have addressed sampling and metamodeling strategy for reservoir simulations. In particular, [26] examines Latin hypercube sampling (LHS) designs and compares polynomial and kriging metamodels, [27] focuses specifically on LHS designs, [28] compares polynomial, kriging, thin plate spline, and artificial neural network metamodels. In [29], the authors compared a second order polynomial model and kriging model using an orthogonal array (OA) sample design in a gas coning case study. In this case, the second order polynomial outperformed kriging with a 36-run design in 14 variables. Ref. [30] settled on first order polynomial models for fitting outputs of a CMG STARS simulation for CO_2 sequestration in deep saline carbonate aquifers. The models were fit using LHS designs of size 100 over 16 variables. Finally, [31] used a Box-Behnken design and a stepwise quadratic regression model to develop probability distributions for responses related to CO_2 injection into deep saline formations.

The goal of this study was to compare two different approaches to sampling and proxy modeling for CO_2 sequestration where a compositional simulator, CMG-GEM, is used as the full-physics model. Running a simulation requires the specification of nine input parameters, and results in a host of responses over a 30-year period. Of these responses, three were chosen for the proxy model comparison. The first is average pressure in the reservoir, the second is radius of the CO_2 plume, and the third is total storage efficiency of the reservoir. All responses were selected at the end of the 30-year period.

2.3.2 Methodology

One of the standard proxy modeling approaches used in the reservoir modeling literature is quadratic polynomial modeling with a classical experimental design. A popular design for this purpose is the Box-Behnken design [25], which assigns a "Low" (-1), "Medium" (0), and "High" (+1) level to each input variable. Levels of the inputs are judiciously chosen in such a way that linear and quadratic terms of the polynomial surface can be estimated with the smallest number of runs possible. This corresponds to a selection of uniquely located sampling points along the edges of a hypercube in the input space (see Fig. 2-12).

X1	X2	X3
-1	-1	0
-1	0	-1
-1	0	+1
-1	+1	0
0	-1	-1
0	-1	+1
0	0	0
0	+1	-1
0	+1	+1
+1	-1	0
+1	0	-1
+1	0	+1
+1	+1	0
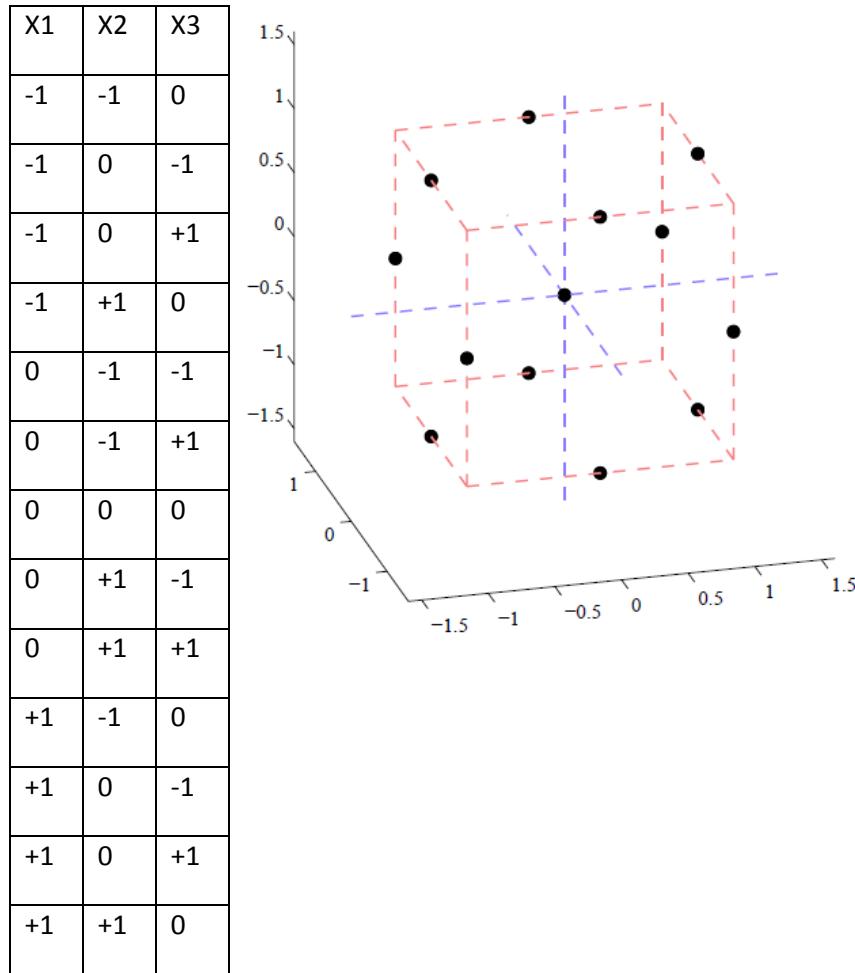
Fig. 2-12. A Box-Behnken Design for three inputs (left) and its representation in the input space (right).

The quadratic polynomial model fits a model to the response that is the analogue of the parabola in p dimensions, where p is the number of inputs. It is defined as a sum of all linear, quadratic, and pair-wise cross-product terms between the predictors. That is, the approximating function $\hat{f}(\mathbf{x})$ is given by the equation below.

$$\hat{f}(\mathbf{x}) = b_0 + \sum_{i=1}^{p} b_i x_i + \sum_{i=1}^{p} b_{ii}(x_i)^2 + \sum_{i=1}^{p} \sum_{j>i} b_{ij} x_i x_j \qquad (2\text{-}10)$$

For responses that have smooth, well-defined behavior over the input space, a quadratic polynomial model based on a classical experimental design like the Box-Behnken design would be appropriate. However, in some cases this may not be a valid assumption. Additionally, interesting behavior in the response could be occurring somewhere between the "Low" and "Medium" input settings, or between the "Medium" and "High" settings. A design which only considers those three input levels may be oversimplifying and not provide an appropriate level of granularity.

An alternate approach is to use a sampling-based design, which is not restricted to three input levels. Such a design generates a sample that is intended to satisfy a particular criterion. In some cases, these designs are even determined through numerical optimization of that criterion. Typically, the criteria capture information about the "space-filling" nature of the design. That is, they measure how well dispersed the sample points are across the input space. Intuitively, the better spaced the points are throughout the space, the fewer "gaps" or "holes" there will be for which no sampled observations were collected at a similar set of input values.

These designs come in many flavors, but the one discussed in the context of this study is a maximin Latin Hypercube sample (LHS) [25]. A LHS is a design that is intended to fill the input space by randomly selecting observations in equal probability bins across the range of the inputs. These designs sample values in [0, 1] for each of the inputs at each design point. The sampling is done in such a way that for a sample of size n, there will be exactly one observation in each of the intervals [0, 1/n], [1/n, 2/n), …, [(n-1)/n, 1] for each of the inputs. A maximin LHS is created by generating a large number (e.g., thousands) of LHS designs and selecting the design that has the largest value of the function

$$M(x^1, x^2, …, x^n) = min_{i,j} \left\| x^i - x^j \right\|, \quad (2\text{-}11)$$

where $\mathbf{x}^1, \mathbf{x}^2, …, \mathbf{x}^n$ are the n sampled observations and $\left\| x^i - x^j \right\|$ is the Euclidean distance between observations i and j. In other words, the maximin LHS design is the one that maximizes the minimum distance between any pair of observations in the sample. Examples of LHS and maximin LHS designs are shown in Fig. 2-13, that highlight the superior space-filling nature of the latter scheme.
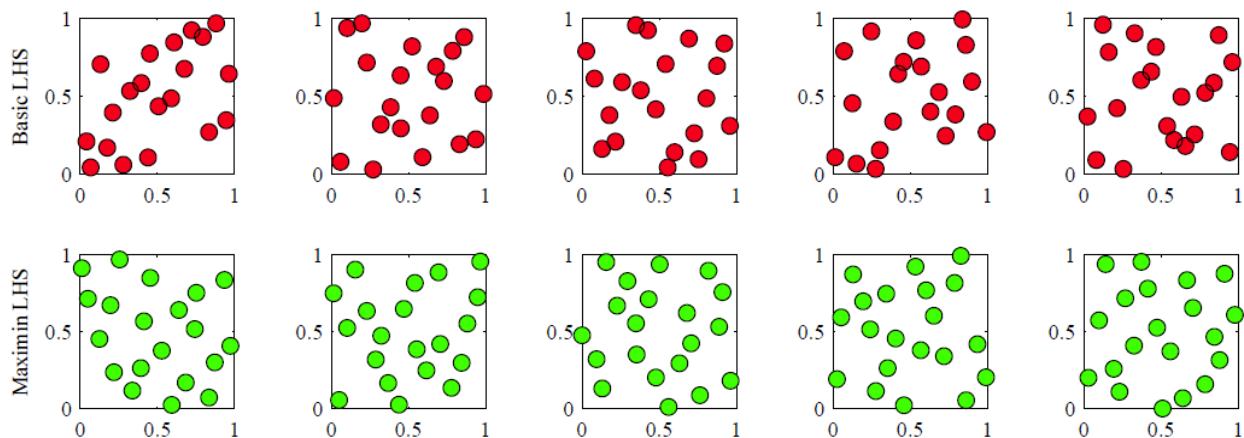

Fig. 2-13. Examples of LHS designs (red) and maximin LHS designs (green) using 20 observations for two inputs.

In addition to sampling designs, there are also alternative proxy models that can be used in place of a quadratic polynomial [32]. A common alternative used for oil and gas applications is the kriging model [32-35], which has an approximation function $\hat{f}(\mathbf{x})$ that is composed of a trend term and an autocorrelation term:

$$\hat{f}(\mathbf{x}) = \mu(\mathbf{x}) + Z(\mathbf{x}), \quad (2\text{-}12)$$

where $\mu(\mathbf{x})$ is the overall trend and $Z(\mathbf{x})$ is the autocorrelation term. $Z(\mathbf{x})$ is treated as the realization of a mean zero stochastic process with a covariance structure given by $Cov(Z(\mathbf{x})) = \sigma^2 \mathbf{R}$, where R is an n×n matrix whose $(i,j)^{\text{th}}$ element is the correlation function $R(\mathbf{x}^i, \mathbf{x}^j)$ between any two of the sampled observations $\mathbf{x}^i$ and $\mathbf{x}^j$. One choice is the Matérn (5/2, θ) correlation, which is given by the equation below, where

$$d_k = \left(x_k^i - x_k^j \right).$$

$$R(\mathbf{x}^i, \mathbf{x}^j) = \prod_{k=1}^{p} \left[1 + \frac{d_k \sqrt{5}}{\theta_k} + \frac{5 d_k^2}{\theta_k^2} \right] exp\left(-\frac{d_k \sqrt{5}}{\theta_k} \right) \qquad (2\text{-}13)$$

In this study, we have used ordinary kriging which assumes a scalar trend $(\mathbf{x}) = \mu_0$,

2.3.3   Study Description

As described previously for the simplified-physics based modeling case, the system being studied represents a single-well injecting supercritical CO₂ into a bounded 2-D radial-cylindrical formation (storage reservoir) initially filled with brine. The model domain consists of a porous and permeable heterogeneous reservoir, overlain by a low-permeability cap rock. The top of the cap rock, the bottom of the reservoir and the lateral boundary are all assumed to be no-flow boundaries. The simulations are executed in the numerical simulator CMG-GEM. Table 2-1 shows the nine independent variables, and the reference (0), low (-1) and high (+1) values used to set up the Box-Behnken designs. Table 2-2 shows the distributions used to sample these variables for the maximin LHS design. Here, T denotes a triangular distribution, and lnT denotes a log-triangular distribution.

Proxy models were trained for each of three responses (total storage efficiency, plume radius and average reservoir pressure) generated by the GEM reservoir simulator. Both sampling designs contained n = 97 runs with different values for the nine input variables. The selection of 97 runs was made because the Box-Behnken design for p = 9 input variables has n = 97 unique observations. To avoid any bias that could be attributed to unequal sample sizes, all of the maximin LHS designs were restricted to the same number of runs as the Box-Behnken design.

Table 2-2. Input Distributions used with LHS Sampling

Input	Description	Distribution
h_R	Thickness of the reservoir, m	T(50,150,250)
h_{CR}	Thickness of the caprock, m	T(100,150,200)

μ_{lnk_R}	Log-mean reservoir permeability (mD),	$\mu_{lnK\_R} \sim T(2.45, 3.56, 4.67)$
V_{DP}	Dykstra-Parson's coefficient (perfectly correlated)	$V_{DP} \sim T(0.35, 0.55, 0.75)$
k_{CR}	Average horizontal permeability of the caprock, mD	$\ln T(0.002, 0.02, 0.2)$
k_V/k_H	Anisotropy ratio	$\ln T(0.01, 0.1, 1)$
q	CO₂ injection rate, MMT/yr	discrete with equal probability – {0.33, 0.83, 1.33}
φ_R	Porosity of the reservoir	$T(0.08, 0.12, 0.18)$
φ_{CR}	Porosity of the caprock	$T(0.05, 0.07, 0.10)$
I_k	Order of permeability layering	Discrete w/equal probability, $I_k \in$ {"random", " increasing", "decreasing"}

To compare different models, the common approach of characterizing the goodness-of-fit based on the training data set was used as a starting point. Note that in this case, the statistics will be biased optimistically, since the metamodel first and foremost is designed to fit those particular observations well. An overtrained model will fit the training data very well, but perform poorly on independent test data. Therefore, an independent ordinary LHS design with m = 97 independent observations was generated as a "validation" data set. Finally, a k-fold cross-validation approach was applied [36].

Under this paradigm, the dataset is randomly partitioned into k folds, which are mutually exclusive and exhaustive subsets of the observations. Each fold is then systematically held out and the metamodel is fit to a dataset consisting of only the remaining k – 1 folds. This model is then used to make a prediction on the fold that was left out. After repeating this process on all k folds, there are a total of k models that are constructed, each of which are used to predict the value of the single fold that was left out of the training set. While the cross-validation approach does not specifically test the unique model that is created by using all n training observations together, it does test the algorithm that is used to construct the model. When each fold is held out of the training set, it will behave like independent test data as far as that particular model is concerned. Therefore, the errors from the cross-validation more accurately reflect error rates in the model fit over parts of the response surface that have not been sampled. The rule of thumb is to use somewhere between k = 5 and k = 10 [36].

The accuracy of each model (using the training data set, independent validation data set, or k-fold cross-validation) was then captured using three different related measures. The first is the root mean squared error (RMSE), which is defined as the square root of the average squared difference between predictions $\hat{y}_i = \hat{f}(\mathbf{x}^i)$ and true response values $y_i = f(\mathbf{x}^i)$ over the set of validation observations $\{\mathbf{x}^1, \mathbf{x}^2, ..., \mathbf{x}^n\}$. The RMSE may also be divided by the median response to produce a scaled RMSE (SRMSE) that

facilitates easier comparison between responses. The final statistic used in model evaluation was a pseudo-R^2 value, which measures the amount of variation in the response that can be attributed to the predictors. Note that in this definition of the R^2 value, negative values are possible and indicate a model that is less useful in prediction than simply using the mean response.

2.3.4   Results

The performance of the two design-model combinations studied, i.e., Box Behnken (BB)-quadratic and maximin (MM)-kriging, are shown in Fig. 2-14. The bar charts show the pseudo-R2 statistic indicating goodness-of-fit for the full training data, independent validation data and k-fold cross-validation exercise. Taller bars indicate better performance. Beginning with the left panel, which shows model performance for the training data only, it is clear that the bars represent a biased view of model performance, since the models are being evaluated over the same dataset used to train them. For example, since kriging models are perfect interpolators (i.e., they pass through each observation by design), they always achieve zero error over the training set. However, one obviously could not expect them to perfectly model the response at other points in the input space. The middle panel shows results for validation using the independent LHS sample set. Here, the performance of BB and MM designs are essentially equivalent when considered across all three metrics.

The right panel shows the results for the cross validation exercise. The question of interest here is: had validation data not been available, would cross-validation have given similar results in terms of which metamodels had the best performance on each of the responses? To investigate this question, a 5-fold cross-validation procedure was implemented 100 times for each of the metamodels. For each response, this produced 100 cross-validated predictions at every set of sampled predictor inputs. The metamodels were compared using the average R^2 over the 100 sets of predictions. There are several interesting things to note in comparing these results to the validation results. First of all, the cross-validation error rates seem higher than the validation error rates, especially for the Box-Behnken design. This is likely because predictions by cross-validated models can only be made at sampled locations in the response surface. In the case of the BB designs, the only samples points were on the boundaries of the predictor space, where models are not as likely to fit well, especially when those points are left out of the training process. These considerations do not apply to space filling designs, because of which the MM LHS appears to be superior to the BB design.
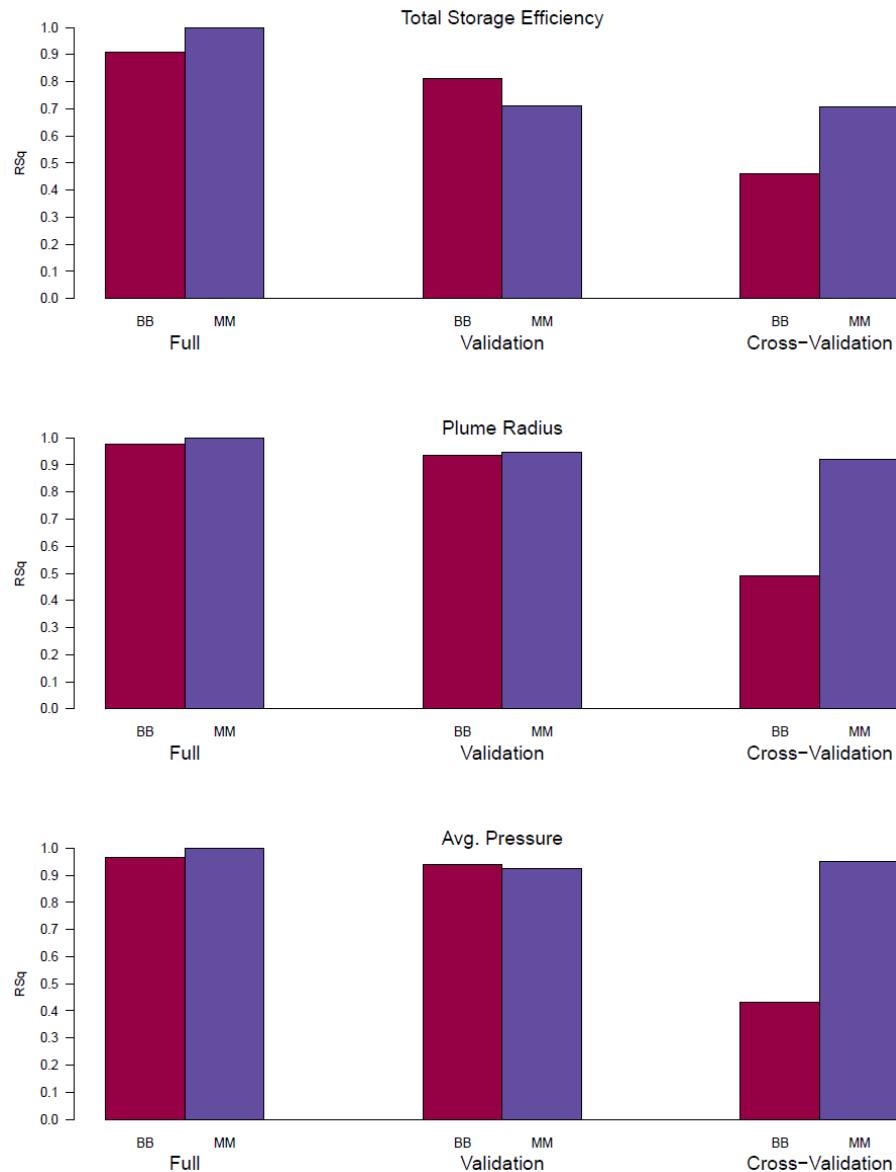
Fig. 2-14. Comparison of R² for BB-quadratic and MM-kriging proxy models for the three different performance metrics of interest.

These results are further substantiated via the scatterplots between the simulated and predicted values of the three performance metrics of interest, shown in Fig. 2-15 through 2-17. These scatterplots show a comparison of the actual response (horizontal axis) to the predicted response (vertical axis), with perfect prediction represented by the dashed diagonal gray line. In the case of the full training evaluation, the dots represent the design used to train the model, with predictions being made on those same design points. In the case of the validation approach, the dots represent the validation LHS design over which the models were evaluated. Finally, in the case of cross-validation, the dots represent the median cross-validated predictions over the training design. The bars show the spread of the predictions over the 100 replications of the cross-validation procedure, with the black line showing the middle 50% of predictions, the dark gray extending out to the 5th and 95th percentile predictions, and the light gray lines extending to the minimum and maximum predicted value. In some cases, the light gray lines are truncated to avoid

distorting the vertical axis. Note also both models tended to underestimate the magnitude of the largest average pressures for the validation set as well as for the cross-validation case.
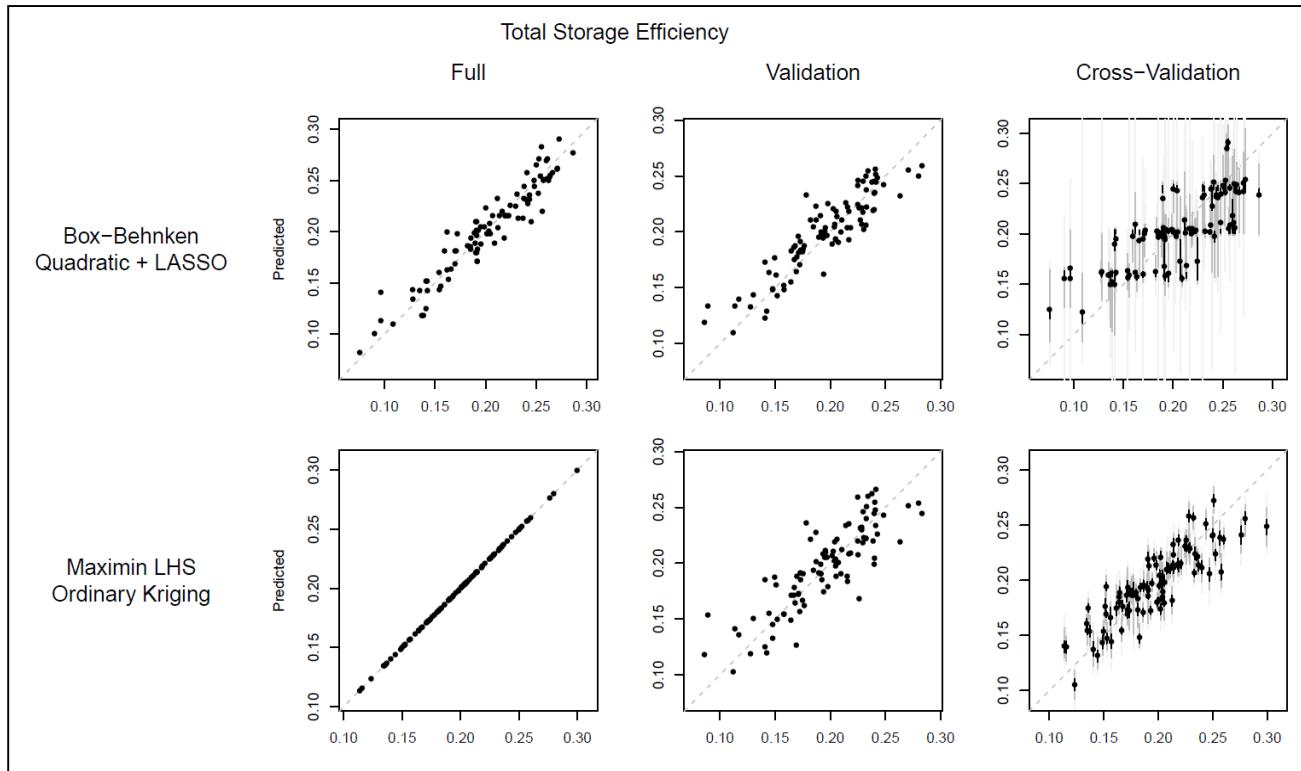
Fig. 2-15. Scatterplots showing actual (horizontal axis) vs. predicted response (vertical axis) for Total Storage Efficiency.
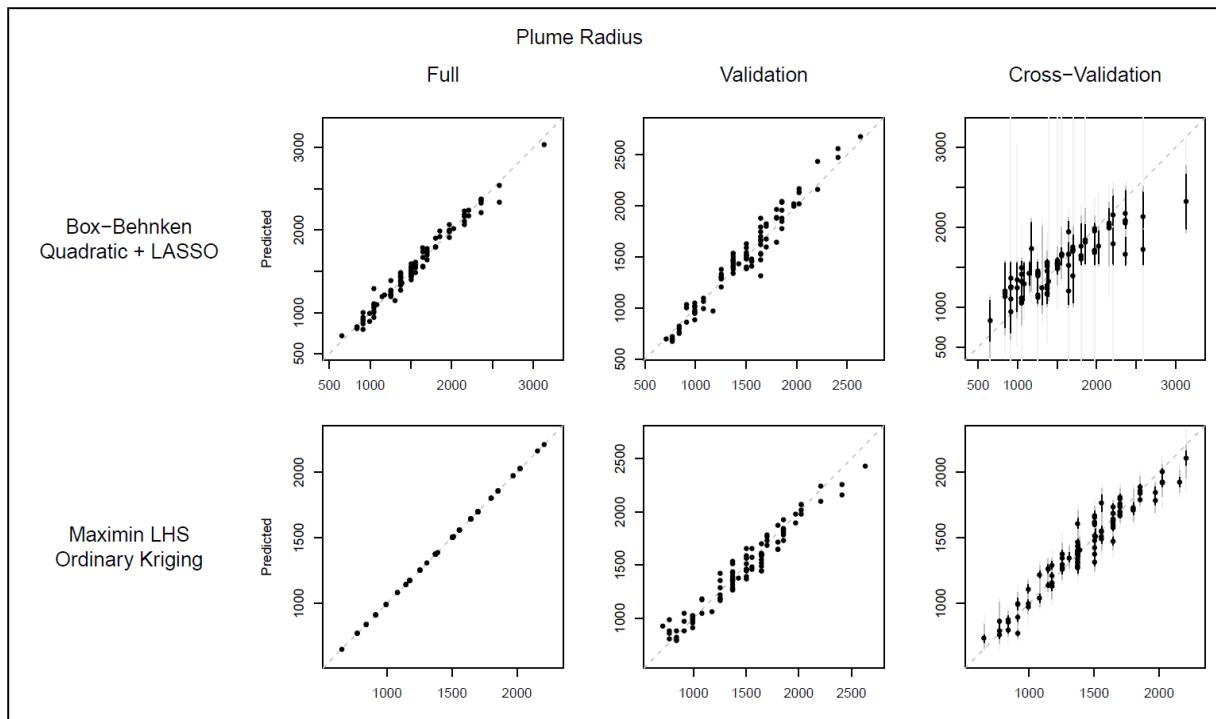
Fig. 2-16. Scatterplots showing actual (horizontal axis) vs. predicted response (vertical axis) for Plume Radius.
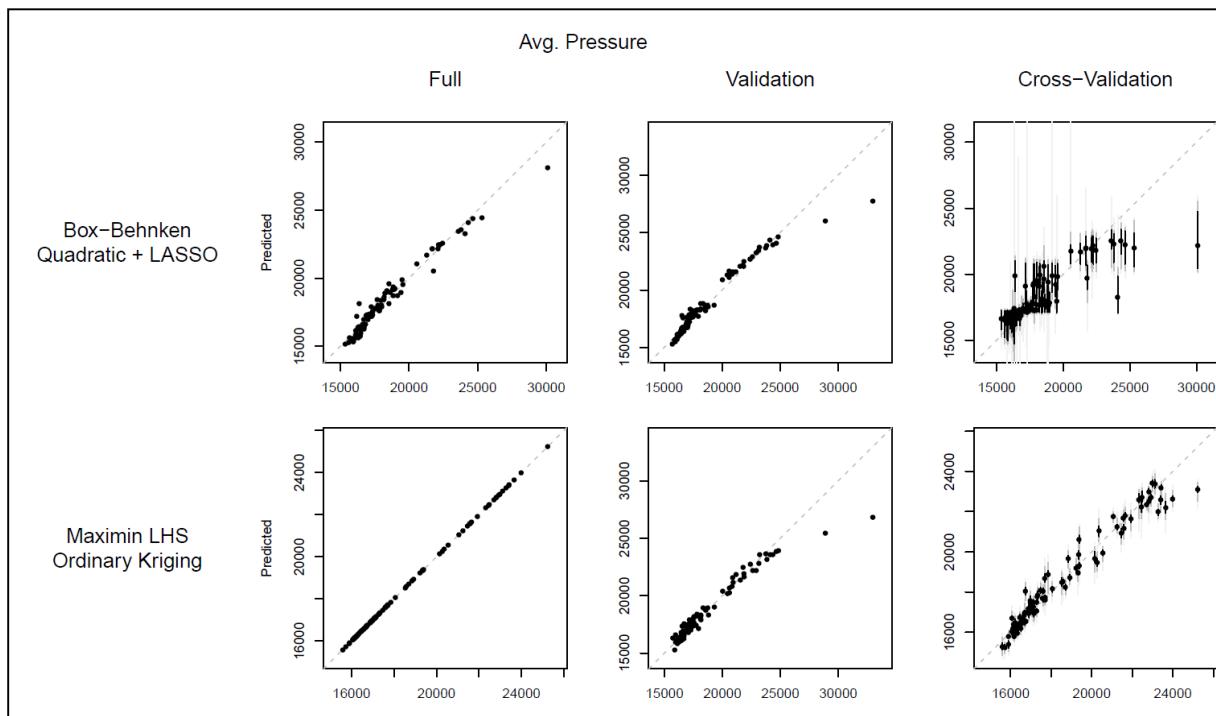
Fig. 2-17. Scatterplots showing actual (horizontal axis) vs. predicted response (vertical axis) for Average Pressure.

2.4 Reduced-Order Method Based Models

2.4.1 Background

Our goal in this work was to develop and test a reduced-order modeling framework for CO_2 storage problems. The method we are pursuing is based on trajectory piecewise linearization (TPWL) and uses proper orthogonal decomposition (POD) to project the linearized representation into a low-dimensional space. We thus refer to the overall method as POD-TPWL. Reduced-order modeling techniques that rely on POD alone have been developed for subsurface flow simulation [37-39], though these methods are limited in terms of the amount of speedup achievable for general (nonlinear) problems such as those associated with CO_2 storage. The TPWL method, originally presented in [40], is more approximate but it can achieve much greater speedups for such cases. Implementations of POD-TPWL for subsurface flow have been reported for oil-water problems [41-42], idealized thermal simulation systems [43], and oil-gas compositional problems [44].

2.4.2 Methodology

The reduced-order model (ROM) developed in this work can be classified as a reduced numerical procedure. As such, it is based on the underlying (discretized) equations describing the flow process of interest. This is in contrast to surrogate models that apply statistical or data-fitting procedures such as those described in previous sections, which are not based directly on the underlying equations.

The governing equations for two-phase or compositional flow in porous formations are derived by combining expressions for mass conservation with Darcy's law. These equations are solved numerically in this work using a fully-implicit finite-volume technique. We apply the usual discretization procedures (two-point flux approximation, first-order implicit time-discretization method, standard well representation), in order to arrive at the discretized flow equations. We then write the nonlinear set of discretized equations (for either black-oil or compositional systems) as:

$$\mathbf{g}(\mathbf{x}^{n+1}, \mathbf{x}^n, \mathbf{u}^{n+1}) = \mathbf{0} \,, \tag{2-14}$$

where g designates the vector of discretized residual equations we wish to solve, x denotes the system states (e.g., pressure and saturation in every grid block in a two-phase flow problem), u designates the specified controls (well bottomhole pressures or injection/production rates), and n and n+1 indicate time levels. The goal is to compute $\mathbf{x}^{n+1}$, the states at the next time level. Previous states $\mathbf{x}^n$ and controls $\mathbf{u}^{n+1}$ are known or specified. This nonlinear system of equations is typically solved iteratively, using Newton's method, which can be very time consuming for large models. For a two-component model containing n_b grid blocks, Eq. 2-14 represents a system of $2n_b$ equations and $2n_b$ unknowns.

In TPWL procedures, the nonlinear set of equations is linearized around "points" (vectors of states and controls) that have been simulated in previous full-order "training" simulations. Given the current state x_n, we designate the closest saved state encountered during the training run as x_i (the specific definition of "distance," used to determine "closeness," is problem dependent; see, e.g., He and Durlofsky [44] for detailed discussion). To determine $\mathbf{x}^{n+1}$, we linearize Eq. 2-14 around the saved states and controls $(\mathbf{x}^{i+1}, \mathbf{x}^i, \mathbf{u}^{i+1})$, and then represent new solutions using the linear expansion

$$\mathbf{g}^{n+1} = \mathbf{g}^{i+1} + \frac{\partial \mathbf{g}^{i+1}}{\partial \mathbf{x}^{i+1}}\left(\mathbf{x}^{n+1} - \mathbf{x}^{i+1}\right) + \frac{\partial \mathbf{g}^{i+1}}{\partial \mathbf{x}^{i}}\left(\mathbf{x}^{n} - \mathbf{x}^{i}\right) + \frac{\partial \mathbf{g}^{i+1}}{\partial \mathbf{u}^{i+1}}\left(\mathbf{u}^{n+1} - \mathbf{u}^{i+1}\right), \qquad (2\text{-}15)$$

where $\mathbf{g}^{n+1} = \mathbf{g}(\mathbf{x}^{n+1}, \mathbf{x}^{n}, \mathbf{u}^{n+1}) = \mathbf{0}$ and $\mathbf{g}^{i+1} = \mathbf{g}(\mathbf{x}^{i+1}, \mathbf{x}^{i}, \mathbf{u}^{i+1}) = \mathbf{0}$. Note that the Jacobian matrix, which is the derivative of the residual vector with respect to the state vector, for time step i+1 in the training run, is given by $\mathbf{J}^{i+1} = \partial \mathbf{g}^{i+1}/\partial \mathbf{x}^{i+1}$. In all of our expressions, this matrix is always evaluated at the converged states $\mathbf{x}^{i+1}$.

Application of POD enables us to represent the states x in terms of a small number of parameters. This is accomplished using the relationship $\mathbf{x} = \mathbf{\Phi}\boldsymbol{\xi}$, where $\mathbf{\Phi}$ is the so-called basis matrix (constructed from "snapshots"; i.e., the solution states computed in training runs) and $\boldsymbol{\xi}$ is the reduced-variable vector. The matrix $\mathbf{\Phi}$ is "tall and skinny," of dimensions 2nb×l, where l << 2nb. This means that the states x (of dimension 2nb) can be expressed efficiently in terms of the "short" vector $\boldsymbol{\xi}$ (of dimension l). After manipulating Eq. 2-15, and inserting $\mathbf{x} = \mathbf{\Phi}\boldsymbol{\xi}$, we have an over-determined system of 2nb equations (for a two-component problem) in l unknowns. This can be written concisely as:

$$\mathbf{J}^{i+1}\mathbf{\Phi}\boldsymbol{\xi}^{n+1} = \mathbf{b}. \qquad (2\text{-}16)$$

Eq. 2-16 must be solved for $\boldsymbol{\xi}^{n+1}$. Information in the right-hand side vector b is known (it is either prescribed or involves information at time step n). See He and Durlofsky [44] and Jin [45] for details.

In order to render Eq. 2-16 directly solvable, it must be projected into a subspace of dimension l. This is accomplished by premultiplying Eq. 16 by a matrix $\left(\mathbf{\Psi}^{i+1}\right)^{T}$, where $\mathbf{\Psi}^{i+1}$ is of the same dimensions (2nb×l) as $\mathbf{\Phi}$. Then, at each time step, the POD-TPWL equation to be solved for $\boldsymbol{\xi}^{n+1}$ is as follows:

$$\left(\left(\mathbf{\Psi}^{i+1}\right)^{T}\mathbf{J}^{i+1}\mathbf{\Phi}\right)\boldsymbol{\xi}^{n+1} = \left(\mathbf{\Psi}^{i+1}\right)^{T}\mathbf{b}. \qquad (2\text{-}17)$$

This equation can be written as $\mathbf{A}_{r}\boldsymbol{\xi}^{n+1} = \mathbf{b}_{r}$, where $\mathbf{A}_{r} = \left(\mathbf{\Psi}^{i+1}\right)^{T}\mathbf{J}^{i+1}\mathbf{\Phi}$ and $\mathbf{b}_{r} = \left(\mathbf{\Psi}^{i+1}\right)^{T}\mathbf{b}$. Note that the dimension of the reduced matrix $\mathbf{A}_{r}$ is l×l, which is much smaller than that of the full-order Jacobian matrix $\mathbf{J}$. This reduction, combined with the fact that we now solve a linear equation, gives POD-TPWL its high degree of efficiency.

The choice for the premultiplication matrix (which is referred to here as the constraint reduction matrix) can have a significant impact on POD-TPWL stability and accuracy for many problems, including CO₂ sequestration. The schemes considered in this study include: (a) Galerkin projection, where we set $\mathbf{\Psi}^{i+1} = \mathbf{\Phi}$, (b) Petrov-Galerkin projection (used within the context of reduced-order modeling by, e.g., Carlberg et al. [46]), where we take $\mathbf{\Psi}^{i+1} = \mathbf{J}^{i+1}\mathbf{\Phi}$, (c) inverse projection (IP), where $\mathbf{\Psi}^{i+1} = \left(\mathbf{J}^{i+1}\right)^{-T}\mathbf{\Phi}$, and (d) weighted inverse projection, which is similar to IP but additionally includes a weighting matrix W to give $\mathbf{\Psi}^{i+1} = \left(\mathbf{J}^{i+1}\right)^{-T}\mathbf{W}^{T}\mathbf{W}\mathbf{\Phi}$.

Stanford's Automatic Differentiation-based General Purpose Research Simulator, AD-GPRS [47], is used for the full-order simulations and to provide all of the state and derivative matrix information required by our POD-TPWL model.

(A) Application of POD-TPWL for 2D Cross-Sectional Model with Vertical Well

The problem we first consider is a cross-sectional (x-z) version of the radial axisymmetric (r-z) model described earlier. Most of the reservoir properties, component properties, fluid properties and rock-fluid properties are consistent between the AD-GPRS model used here and the GEM base case model described previously. There are, however, some discrepancies, e.g., (a) AD-GPRS uses an equation of state to compute gas dissolution into water, rather than Henry's law, as is used in GEM, and (b) the AD-GPRS model does not include salinity, which results in slightly different liquid density and viscosity compared to GEM. The AD-GPRS model does not include capillary pressure effects, and it uses the same relative permeability curve for both the reservoir and cap rock. We inject CO_2 at the same rate as in the GEM base case. The simulation period is 30 years.

As discussed above, the POD-TPWL procedure transforms the high-dimensional nonlinear compositional problem into a linear model with a small number of variables. Once the POD-TPWL model is built using information from training simulations, it is capable of providing fast forecasts for new sets of controls (such as well BHPs). To this end, two training simulations are used; one to provide the linearization points, and the other to provide additional snapshots, which are required to construct the basis matrix. The 2000 full-order pressure variables are reduced to 90 low-dimensional variables, and the 4000 mole fraction variables are reduced to 120 low-dimensional variables. The POD-TPWL model is then used to predict the injection rate and well-block pressure for a new (test) case in which the time-varying injection-well BHP differs from that used in the training run.

Fig. 2-18 shows the time-varying BHPs for the training and test simulations. Both BHPs increase monotonically, but they start at different points and have different slopes. Fig. 2-19 shows the injection-block pressure (left) and CO_2 injection rate (right) results for the various simulations. The black dotted curves represent the solution for the training case, around which we linearize. The red curves represent the true (full-order) solution for the test case, computed using AD-GPRS. The test-case solution clearly differs from the training solution. We run POD-TPWL with three of the constraint reduction methods discussed above. POD-TPWL with Galerkin projection is not stable for this case and the results are not presented here. For injection-block pressure, both the Petrov-Galerkin (PG) method and the inverse projection (IP) method match the true solution closely (both POD-TPWL solutions overlay the AD-GPRS solution), though the IP method provides slightly better accuracy than the PG method.

The improvement in accuracy using the IP method is more apparent in the prediction of the CO_2 injection rate. Here the POD-TPWL-IP results (purple curve) essentially overlay the true AD-GPRS results (red curve). In this case, because of the very high well index, the injection rate is particularly sensitive to small errors in the injection-block pressure, which is why the POD-TPWL-PG results (blue curve) display some inaccuracy. It is significant that the POD-TPWL-IP method is able to provide a high level of accuracy for this important quantity.
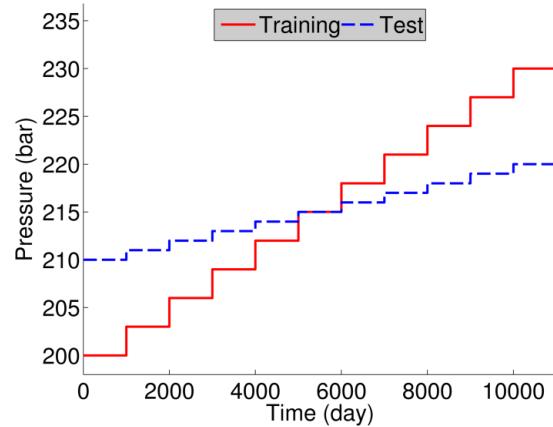
Fig. 2-18. Time-varying BHPs for the training and test cases.
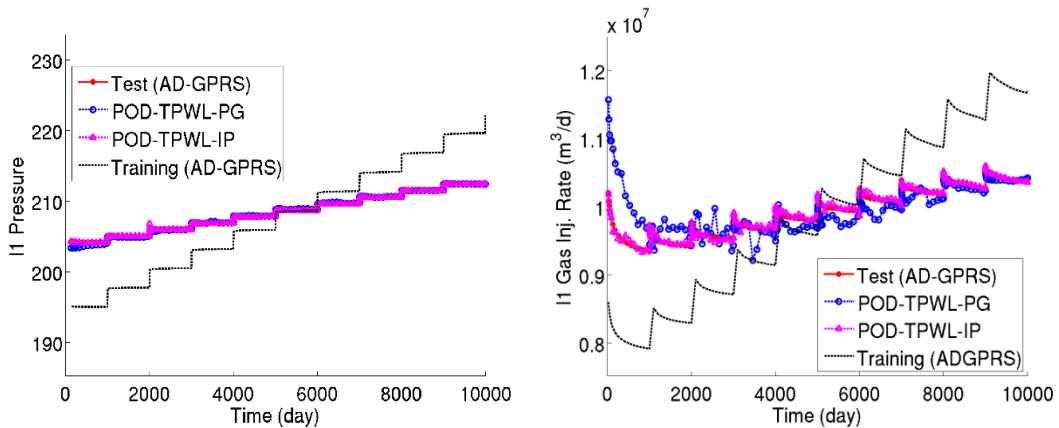
Fig. 2-19. Injection-block pressure (left) and CO$_2$ injection rate (right) for test case.

2.4.3 Application of POD-TPWL for 3D Model with Horizontal Wells

We now describe the application of our POD-TPWL reduced-order modeling framework for an idealized model of CO$_2$ storage in the Mount Simon Sandstone in Illinois. This formation was the target for the CO$_2$ storage associated with FutureGen 2.0 [48]. The model and permeability field, shown in Figs. 2-20 and 2-21, are intended to be conceptual and lack many of the complexities of the simulation model developed and applied at Pacific Northwest National Laboratory. The simplified model used here is nonetheless quite useful for POD-TPWL testing. It represents the storage aquifer on a 30×30×30 grid (total of 27,000 grid blocks), and the full regional system on a 46×46×30 grid (total of 63,480 grid blocks). The storage aquifer is of physical dimensions 3.1 mi (5 km) × 3.1 mi (5 km) × 1346 ft (410 m), and the full model is of dimensions 100 mi × 100 mi × 1346 ft. CO$_2$ injection is accomplished using four horizontal wells, as shown in Fig. 20 (right).

Fig. 2-20. Areal grid and well locations for conceptual Mount Simon model.
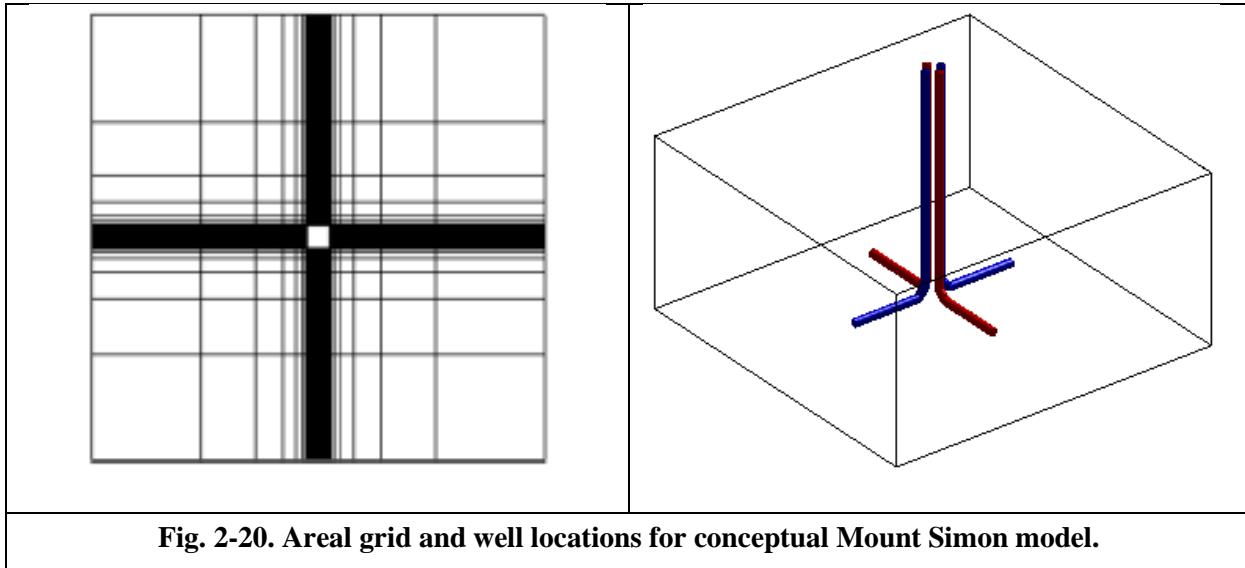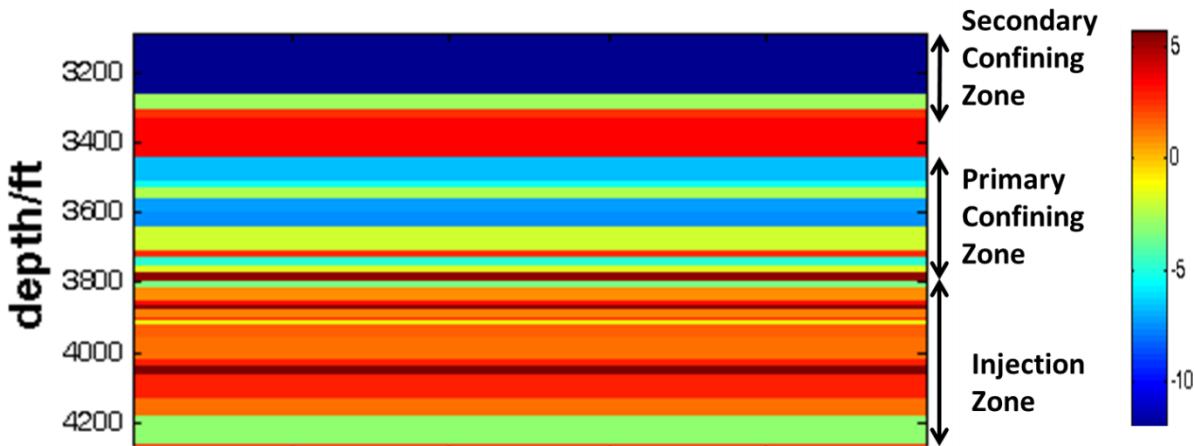
Fig. 2-21. Log horizontal permeability (mD) for conceptual Mount Simon model.

(A) Wells with BHP Control

As explained earlier, in order to apply the POD-TPWL model, we first perform one or more full-order AD-GPRS training runs. Results and data from these runs are used to construct the POD-TPWL model. For test runs, the degree of perturbation from the training run can be quantified using the parameter α, with α=0 indicating the training run and α=1 the case with the largest perturbation, referred to as the target case. For values of α between 0 and 1, the test-case BHP for a particular well at time t (designated u_{test}^t) used in the simulation is computed using:

$$u_{test}^t = (1 - \alpha)u_{training}^t + \alpha u_{target}^t , \qquad (2\text{-}18)$$

where $u_{training}^t$ and u_{target}^t are the training and target BHPs for the well at time t.

Fig. 2-22 shows the time-varying BHPs for the training (α=0) and target (α=1) runs. In the training run, wells I1 and I3 display a decrease in BHP at 4000 days, while wells I2 and I4 display (stepwise-linearly) increasing BHPs. In the target case the trends are the opposite – wells I1 and I3 have increasing BHPs, and wells I2 and I4 have BHPs that decrease at 4000 days. This represents a challenging case for the POD-TPWL model.

Test results for α=0.5 are shown in Fig. 2-23. The red line and points denote the reference (full-order) AD-GPRS simulation results. The blue lines and points are the POD-TPWL results, which are labeled PG_PS_90_120 ("PG" indicates Petrov-Galerkin, which is the constraint reduction procedure used, and "PS_90_120" indicates the number of reduced pressure and mole fraction variables), and the black dotted curves represent training results. The POD-TPWL results are seen to be quite accurate over much of the simulation period, but for times up to about 1000 days, errors relative to AD-GPRS are evident. These errors are most noticeable for wells I2 and I4. In general, we observe these errors to decrease with decreasing values of α.

(B) Wells with Rate Control

A new feature in the current POD-TPWL implementation is the ability to use well rates, rather than BHPs, as the control parameters. See Jin [45] for the implementation details associated with this capability. We now consider results using this type of specification. The rate profiles for the training and test runs are shown in Fig. 2-24. In both cases, all wells are specified to inject the same volume of CO_2, though this is not a requirement of the implementation. Test-case results for injection well BHPs for the four wells are presented in Fig. 2-25. The various curves are as described earlier. The POD-TPWL results in Fig. 2-25 display reasonable accuracy relative to the reference full-order simulation for this challenging problem. There is, however, some inaccuracy at late time (after ~6500 days). We believe this is due to limitations in the current POD-TPWL point selection scheme, and we plan to generalize this procedure in future work. Runtime speedups of about a factor of 370 are achieved using POD-TPWL (relative to the full-order simulation) for this 3D case.

Training case ($\alpha = 0$) Target case ($\alpha = 1$)
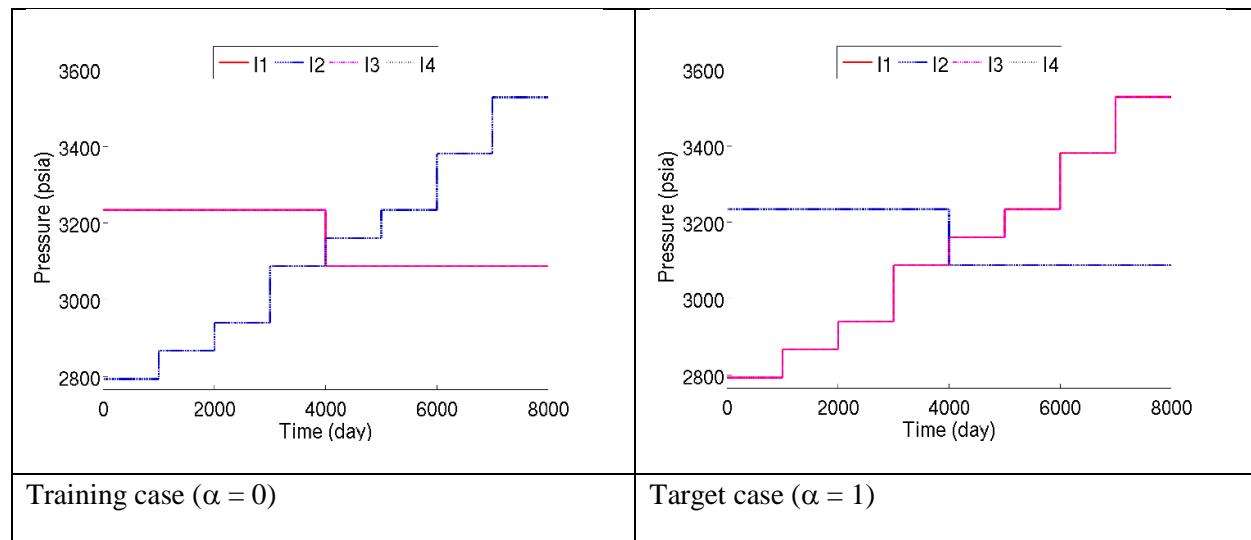
Fig. 2-22. Training and target BHPs for the four injection wells.

Well I1	Well I2
Well I3	Well I4
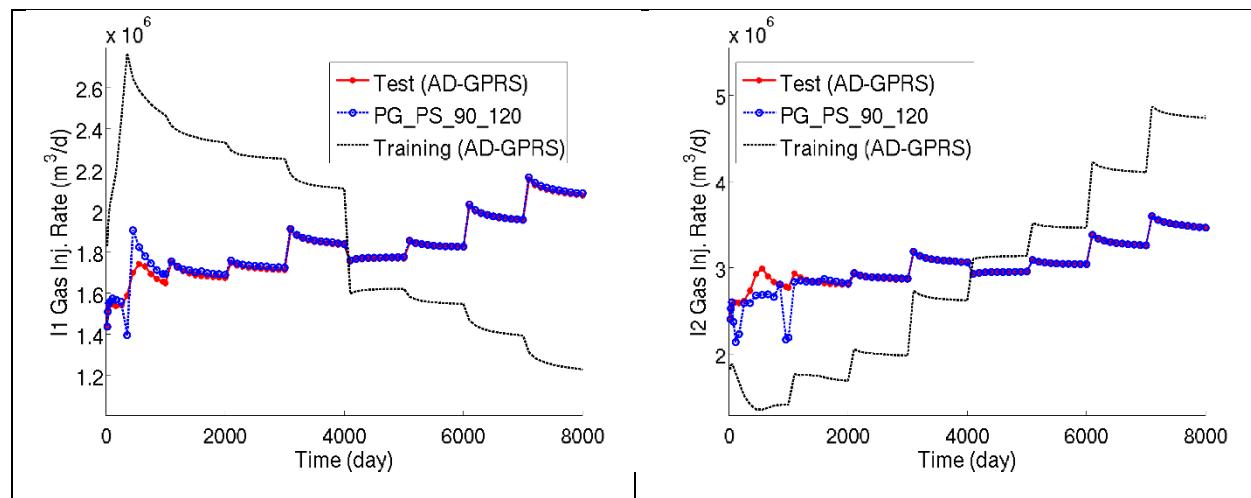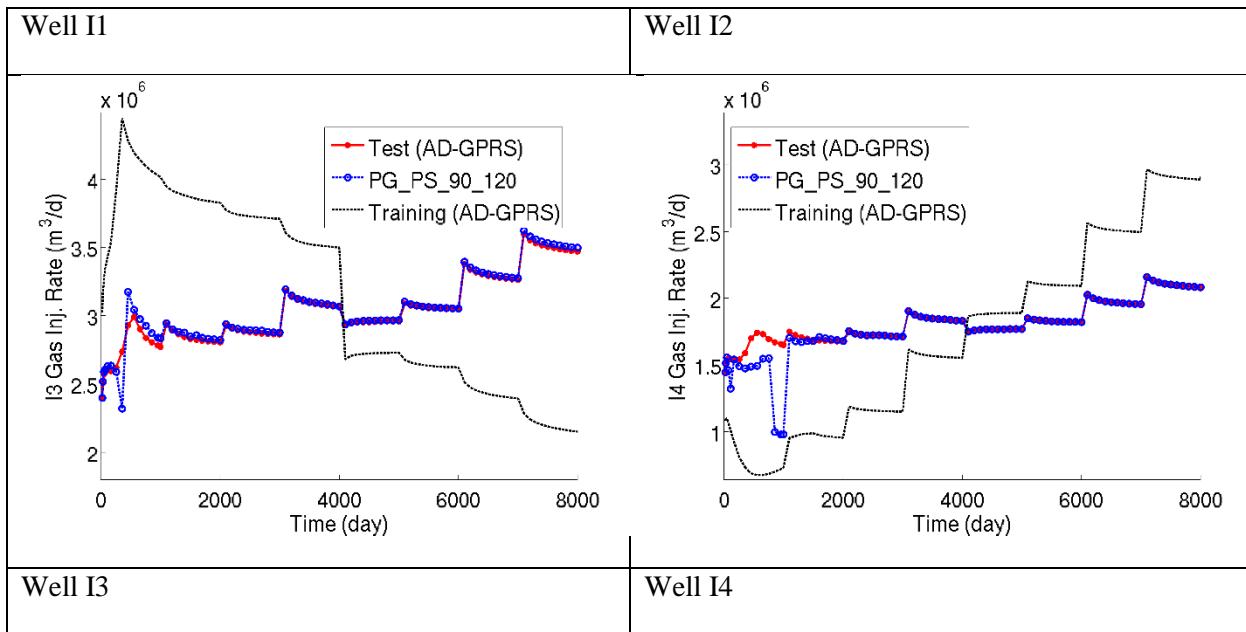
Fig. 2-23. CO₂ injection rates for test case with α = 0.5.

Training case	Test case
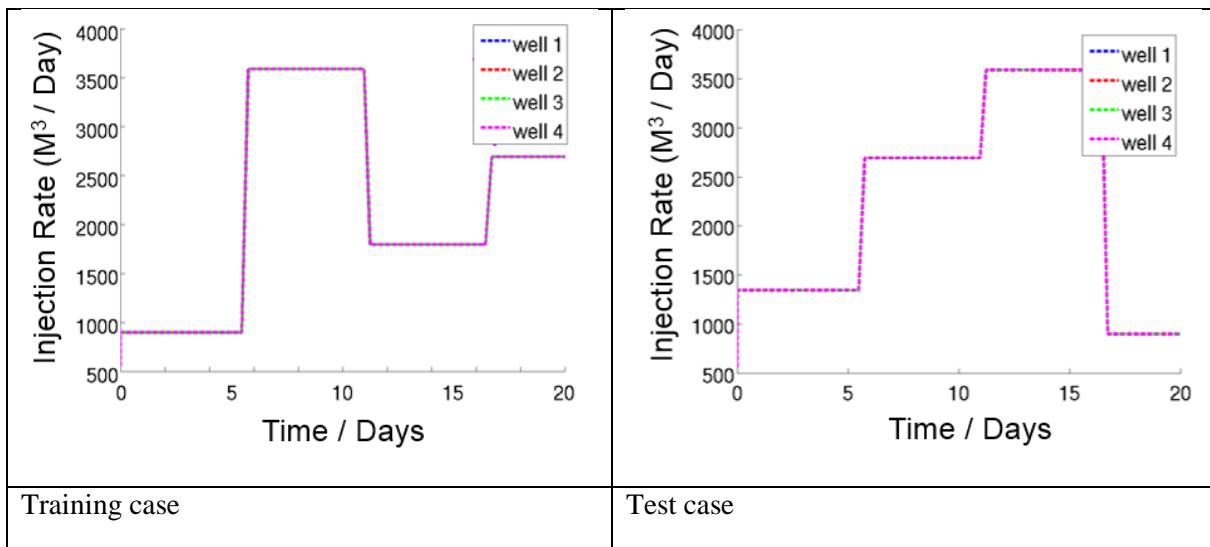
Fig. 2-24. Time-varying rate specifications for training and test simulations.

Well I1

Well I2

Well I3

Well I4
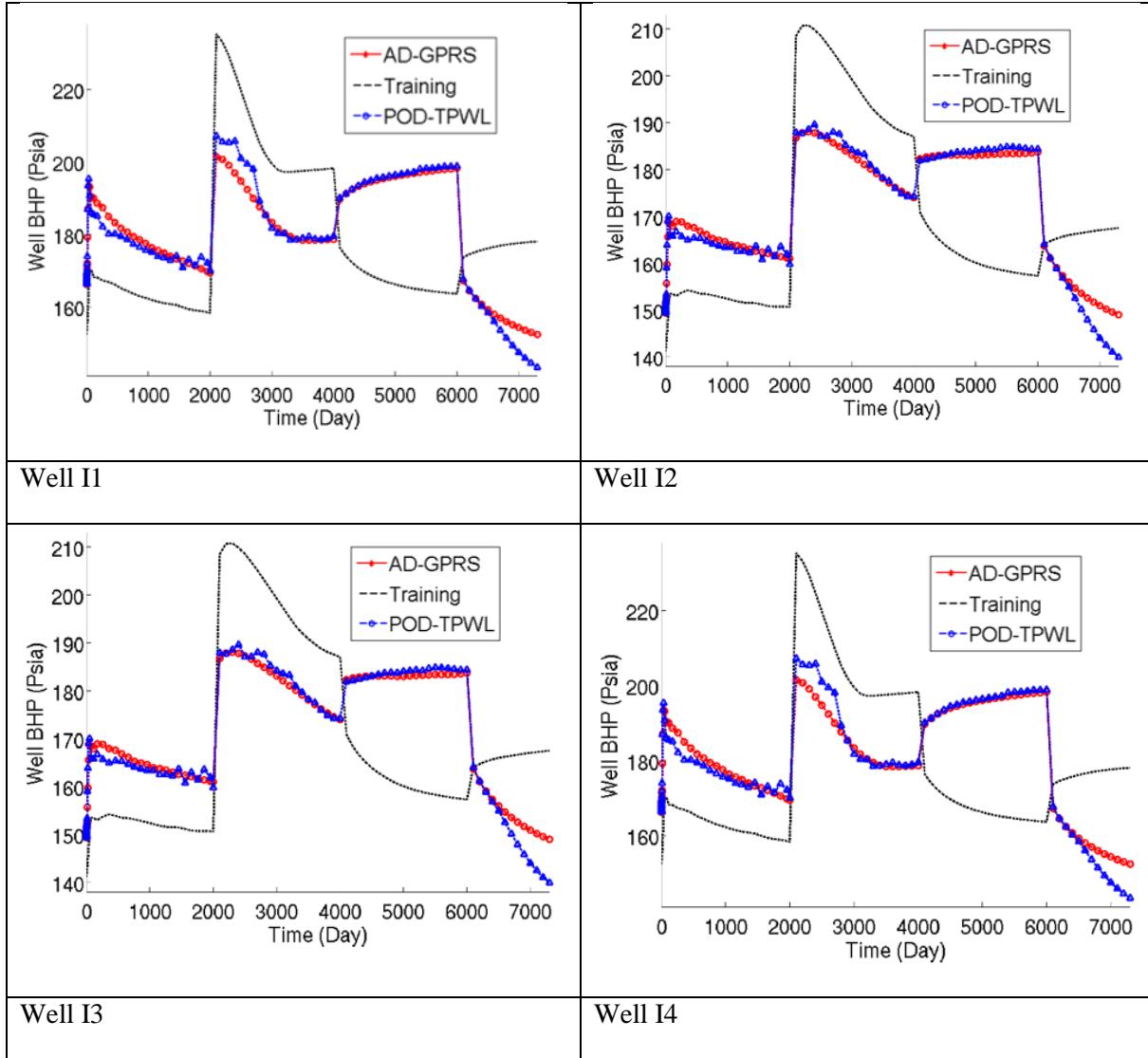
Fig. 2-25. CO₂ injection well BHPs for test case.

(C) Prediction for Cases Involving Geological Perturbation

We now develop POD-TPWL models in which the perturbed "control" variable is a geological parameter. Our discussion here, and the general development, follows that in He et al. [49] and Jin [45], where full details can be found. We define $\gamma = \log T$, where T is the usual block-to-block transmissibility. The new term appearing in the TPWL representation is now:

$$\frac{\partial \mathbf{g}^{i+1}}{\partial \boldsymbol{\gamma}_\omega}(\boldsymbol{\gamma} - \boldsymbol{\gamma}_\omega) = \frac{\partial \mathbf{g}^{i+1}}{\partial \mathbf{T}_\omega}\mathbf{D}_{T_\omega}(\boldsymbol{\gamma} - \boldsymbol{\gamma}_\omega), \qquad (2\text{-}19)$$

where $\mathbf{g}^{i+1}$ denotes the residual vector for the training run, $\mathbf{T}_\omega$ designates the vector of transmissibilities for the training simulation, and $\mathbf{D}_{T_\omega}$ is a diagonal matrix whose elements coincide with $\mathbf{T}_\omega$. The POD-TPWL model now becomes

$$\xi^{n+1} = \xi^{i+1} - \left(\mathbf{J}_r^{i+1}\right)^{-1}[\mathbf{A}_r^{i+1}\left(\xi^n - \xi^i\right) + \widetilde{\boldsymbol{B}}_r^{i+1}(\boldsymbol{\gamma} - \boldsymbol{\gamma}_\omega)] \,. \tag{2-20}$$

Here $\widetilde{\mathbf{B}}_r^{i+1}$ is given by

$$\widetilde{\mathbf{B}}_r^{i+1} = \boldsymbol{\Psi}^T \frac{\partial \mathbf{g}^{i+1}}{\partial \mathbf{T}_\omega} \mathbf{D}_{T\omega} \,, \tag{2-21}$$

where all variables are as defined previously.

We test this procedure on a vertical slice of the Mount Simon model where the storage aquifer is represented by 30×30 grid blocks and the full regional system by 46×30 blocks. CO_2 injection is from two horizontal wells near the bottom of the model, with the injection schedule for both wells given in Fig. 2-26. The training run corresponds to the geological model in Fig. 2-21. The test case involves a model in which all permeabilities (and thus all transmissibilities) are multiplied by a factor of 2.0 relative to the training case.

The POD-TPWL results for the test case are presented in Fig. 2-27. It is apparent that there are only small differences between the (full-order) training and test-case results, though the test-case results are captured by the POD-TPWL model. These results are preliminary, though they do suggest that the POD-TPWL implementation for geological perturbation is essentially correct. Further testing and development of this capability will be the subject of future work.
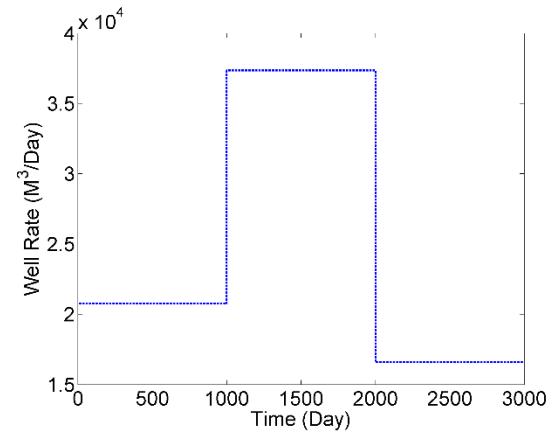
Fig. 2-26. Injection rates for training and test cases.
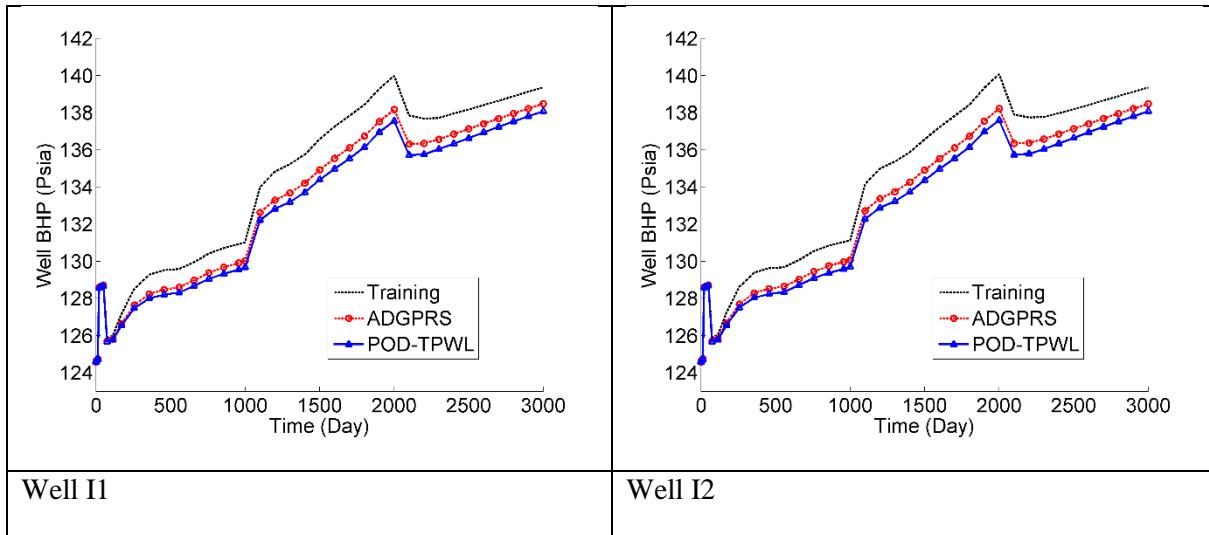
Fig. 2-27. CO_2 injection well BHPs for test case (geological perturbation example).

2.5   Summary and Concluding Remarks

Here, we summarize the findings of the main component of our research project whose objective was to develop and validate a portfolio of simplified modeling approaches for CO_2 sequestration in deep saline formations – based on simplified physics, statistical learning, and/or mathematical approximations – for predicting: (a) injection well and formation pressure buildup, and (b) lateral and vertical CO_2 plume migration. Such computationally-efficient alternatives to conventional numerical simulators can be valuable assets during preliminary CO_2 injection project screening, serve as a key element of probabilistic system assessment modeling tools, and assist regulators in quickly evaluating geological storage projects.

2.5.1   Simplified-physics based models

For the simplified-physics based approach, we have used a set of well-designed full-physics compositional simulations to understand key processes and parameters affecting pressure propagation and buoyant plume migration. Based on these insights, we have developed correlations for dimensionless pressure buildup (injectivity) as a function of the slope of fractional-flow curve, variance of layer permeability values, and the nature of vertical permeability arrangement. The same variables, along with a modified gravity number, can be used to develop a correlation for the total storage efficiency within the CO_2 plume footprint. Similar correlations are also developed to predict the average pressure within the injection reservoir, and the pressure buildup within the caprock. These relationships are thus a hybrid of: (a) first principles and (b) response surface type modeling. The simplification of physics occurs through the sensitivity analysis of full-physics simulations, which helps in isolating the key variables and dimensionless groups affecting the performance metrics of interest. Also, such an approach is useful only when the "macro" behavior of the system is being required, rather than point to point variations in the state variables.

In order to use the predictive models for well injectivity or plume extent, we need to determine the input sources for each of the independent variables involved. The most important terms in the simplified model for total storage efficiency involve the relative permeability model followed by the reservoir heterogeneity. Of the four independent variables, the porosity, thickness (from logs) and permeability are assumed to be known for any given reservoir. Dykstra-Parsons coefficient can be calculated with the knowledge of the permeability distribution in the reservoir obtained from well logs. Typical values of the Dykstra-Parsons coefficient found in literature lie between 0.5 and 0.7. The Lorenz coefficient is related to VDP and can be obtained from knowledge of the spatial arrangement of permeability in the vertical layers. Brine viscosity can be calculated using reservoir salinity, pressure and temperature data. The slope of the tangent to the fractional flow curve is one of the hardest inputs to obtain for a given reservoir. In the absence of core data to test with, we encourage the user to use a lower and upper bound for the df_g/dS_g values from our study. This would yield an expected range of values for the injectivity.

Regarding the average pressure behavior in the reservoir for a given amount of CO_2 injected, we determine that the effectiveness of two-phase flow in a given reservoir depends on an 'f' factor. For closed reservoirs, this 'f' factor (which is a function of the relative permeability) is correlated to the square of the ratio of the reservoir radius to the plume radius at the end of injection. When an overlying cap rock is present, this 'f' factor is modified to account for the relative storage capacity of the rock, i.e.,

ratio of reservoir storativity to the total system storativity. These parameters are readily obtainable from geologic considerations, and by applying our predictive model for plume radius.

2.5.2   Statistical-learning based models

In this strategy, we use statistical learning based methods to build "proxy" or surrogate models that serve as functional equivalents of full-physics simulation results. We have compared two approaches for building a statistical proxy model for CO_2 geologic sequestration from the results of detailed compositional simulations. The first approach involves a classical Box-Behnken experimental design with a quadratic polynomial response surface. The second approach used a space-filling maximin Latin Hypercube sampling combined with an ordinary kriging meta-modeling techniques. Simulations results for CO_2 injection into a reservoir-caprock system with 9 design variables (and 97 samples) were used to generate the data for developing the proxy models. The fitted models were validated with using an independent data set and a cross-validation approach for three different performance metrics: total storage efficiency, CO_2 plume radius and average reservoir pressure.

The performance of the Box-Behnken – quadratic polynomial and the maximin LHS – kriging metamodels are roughly equivalent for the independent validation data set, with the latter clearly performing better for the cross-validation data exercise across all three responses. Thus, the maximin – kriging metamodel can be considered to be a better overall choice for building robust predictive models. The space-filling maximin LHS design provides a higher level of granularity than the 3-point Box-Behnken design, and thus can provide a better understanding of input-output sensitivities at different points in the parameter space. The kriging metamodel is a robust interpolator with many positive qualities, but is computationally expensive to train and predict. Elsewhere, we describe how a quadratic polynomial, combined with a LASSO variable selection scheme, can be an effective alternative to kriging for metamodeling purposes in conjunction with a maximin LHS design [32].

Also note that a single proxy modeling strategy may not necessarily perform in a similar manner for different performance metrics, as indicated by the results for average pressure. This aspect of proxy modeling was also pointed out elsewhere [28]. From a practical standpoint, this may require building different proxy models for each performance metric and evaluating them based on a cross-validation criteria.

2.5.3   Reduced-order method based models

Reduced-order models provide a means for greatly accelerating the detailed simulations that will be required to manage CO_2 storage operations. In this work, we investigated the use of one such method, POD-TPWL, which has previously been shown to be effective in oil reservoir simulation problems. This method combines trajectory piecewise linearization (TPWL), in which the solution to a new (test) problem is represented through a linearization around the solution to a previously simulated (training) problem, with proper orthogonal decomposition (POD), which enables solution states to be expressed in terms of a relatively small number of parameters. In this study, we have applied POD-TPWL for CO_2-water systems simulated using a compositional procedure. Stanford's Automatic Differentiation-based General Purpose Research Simulator (AD-GPRS) performs the full-order training simulations and provides the output (derivative matrices and system states) required by the POD-TPWL method. A new

POD-TPWL capability introduced in this work is the use of horizontal injection wells that operate under rate (rather than bottom-hole pressure) control.

Simulation results were presented for CO_2 injection into a simplified model of the Mount Simon formation. Test cases involved the use of time-varying well controls that differed from those used in training runs. Results of reasonable accuracy were consistently achieved for relevant well quantities. Speedups of around a factor of 370 relative to full-order AD-GPRS simulations were observed for the 3D example. The preprocessing needed for POD-TPWL model construction corresponds to the computational requirements for about 2.3 full-order simulation runs (most of this time is used in performing the two full-order training runs). A preliminary treatment for POD-TPWL modeling in which test cases differ from training runs in terms of geological parameters (rather than well controls) was also presented. Results in this case involved only small differences between training and test runs, though they do demonstrate that the approach is able to capture basic solution trends.

References

1. Benson, S. and Cook, P., 2005. Underground Geological Storage, Carbon Dioxide Capture and Storage, 431 pp., Chapter 5.
2. DOE/NETL, 2010. Carbon Sequestration Atlas III of the United States and Canada.
3. Pruess, K., Xu, T., Apps, J., and Garcia, J., 2003. Numerical modeling of aquifer disposal of CO_2. SPEJ, 49-60 (SPE 83695).
4. Gasda SE, Nordbotten JM, Celia MA. 2012. Application of simplified models to CO_2 migration and immobilization in large-scale geological systems. International Journal of Greenhouse Gas Control, Vol. 9, p. 72–84.
5. Stauffer, P.H, H.S. Viswanathan, R.J. Pawar, M.L. Klasky, and G.D. Guthrie, 2006, CO2-PENS: A CO_2 sequestration systems model supporting risk-based decisions, in Proceedings of the XVI International Conference on Comp. Methods in Water Resources, edited by P. J. Binning et al., Copenhagen, Denmark.
6. Woods, E. G., and Comer, A. G., 1962. Saturation distribution and injection pressure for a radial gas-storage reservoir. Journal of Petroleum Technology 14.12: 1–389.
7. Saripalli KP, and McGrail BP. 2002. Modeling deep-well injection of CO_2 for geological sequestration. Energy Conversion and Management, Vol. 43, p. 185–198.
8. Noh M, Lake LW, Bryant SL, Araque-Martinez A. 2007. Implications of coupling fractional flow and geochemistry for CO_2 injection in aquifers. SPE Reservoir Engineering and Evaluation, Vol. 10(4), p. 406–411.
9. Benson SM. 2003. Pressure buildup at CO_2 injection wells. Second Annual Conference on Carbon Sequestration, Alexandria,VA; 5-8 May.
10. Burton M, Kumar N, Bryant SL. 2008. Time-dependent injectivity during CO_2 storage in aquifers. Paper SPE 113937; SPE/DOE Improved Oil Recovery Symposium, Tulsa, Oklahoma; 19–23 April.
11. Oruganti Y, and Mishra S. 2013. An improved simplified analytical model for CO_2 plume movement and pressure buildup in deep saline formations. International Journal of Greenhouse Gas Control, Vol. 14, p. 49-59; DOI: 10.1016/j.ijggc.2012.12.024.
12. Nordbotten JM, Celia MA, Bachu S. 2005. Injection and storage of CO_2 in deep saline aquifers: analytical solution for CO_2 plume evolution during injection. Transport in Porous Media, DOI: 10.1007/s11242-004-0670-9.
13. M. Dentz and D.M. Tartakovsky. 2009. Abrupt-interface solution for carbon dioxide injection into porous media. Transport in Porous Media, 79(1):15-27.
14. Mathias, S., Hardisty, P., Trudell, M., and Zimmerman, R., 2008. Approximate solutions for pressure buildup during CO_2 injection in brine aquifers. Transport in Porous Media, no. 2. pp. 265–284.
15. Azizi, E., and Cinar, Y., 2013. Approximate analytical solutions for CO_2 injectivity into saline formation. Paper SPE-165575, SPE Reservoir Evaluation & Engineering, May.
16. Zhou, Q., Birkholzer, J., Tsang, C., and Rutqvist, J., 2008. A method for quick assessment of CO_2 storage capacity in closed and semi-closed saline formations. International Journal of Greenhouse Gas Control 2, 626–639.

17. Ehlig-Economides, C. and M. J. Economides, 2010, Sequestering carbon dioxide in a closed underground volume, Journal of Petroleum Science & Engineering, v. 70, no. 1-2, p. 123-130.

18. Sminchak J, White S, Mishra S, Oruganti Y., 2012. CO$_2$ storage simulation results integrating historical injection data and geotechnical information for the Cambrian Mt. Simon sandstone in the Arches province of the Midwest United states. AAPG Eastern Section Annual Meeting, Cleveland, OH; 23–28 September.

19. Sminchak J (ed). 2012. Variable Density Flow Modeling for Simulation Framework for Regional Geologic CO$_2$ Storage along Arches Province of Midwestern United States, Topical Report. 2012. US Dept. of Energy, National Energy Technology Laboratory, Pittsburgh, PA, 124 pp.

20. Zhou Q, Birkholzer JT, Mehnert E, Lin Y-F, Zhang K., 2010. modeling basin- and plume-scale processes of CO$_2$ storage for full-scale deployment, Ground Water, Vol. 48, p. 494–514.

21. Saadatpoor E. 2009. Effect of Capillary Heterogeneity on Buoyant Plumes: New Trapping Mechanism in Carbon Sequestration. MS thesis, Department of Petroleum and Geosystems Engineering, The University of Texas at Austin.

22. Lee, W. J., 1982, Well Testing, Society of Petroleum Engineers, Richardson, TX.

23. Novakovic, D., 2002. Numerical Reservoir Characterization Using Dimensionless Scale Numbers with Application in Upscaling. PhD thesis, Louisiana State University, August.

24. Lake, L.W., 1989. Enhanced Oil Recovery.Englewood Cliffs, New Jersey: Prentice Hall.

25. Santner, T., B. Williams and W. Notz, 2003. The Design and Analysis of Computer Experiments, Springer Verlag, New York, 2003.

26. Osterloh, W. 2008. Use of multiple-response optimization to assist reservoir simulation probabilistic forecasting and history matching. In SPE Annual Technical Conference and Exhibition.

27. Ekeoma, E. and D. Appah. 2009. Latin hypercube sampling (LHS) for gas reserves. In Nigeria Annual International Conference and Exhibition.

28. Zubarev, D. 2009. Pros and cons of applying proxy-models as a substitute for full reservoir simulations. In SPE Annual Technical Conference and Exhibition.

29. Kalla, S. and C.D. White. 2005. Efficient design of reservoir simulation studies for development and optimization. In SPE Annual Technical Conference and Exhibition.

30. Anbar, S., 2010. Development of a predictive model for carbon dioxide sequestration in deep saline carbonate aquifers. In SPE Annual Technical Conference and Exhibition.

31. Wriedt, J., et al., 2014. A methodology for quantifying risk and likelihood of failure for carbon dioxide injection into deep saline reservoirs. International Journal of Greenhouse Gas Control, 20: p. 196–211.

32. Schuetter, J., S. Mishra and D. Mooney, 2014. Evaluation of metamodeling techniques on a CO$_2$ injection simulation study. Proc., 7th International Congress on Environmental Modeling & Software, San Diego, CA, 6-9 June.

33. Simpson, T.W., et al., Comparison of response surface and kriging models for multidisciplinary design optimization. AIAA paper 98, 1998. 4758(7).

34. Cressie, N., 1993. Statistics for Spatial Data (Wiley series in probability and statistics).

35. Krige, D.G., 1951. A statistical approach to some mine valuation and allied problems on the Witwatersrand, University of the Witwatersrand.

36. Hastie, T., R. Tibshirani, and J.H. Friedman, 2008. The Elements of Statistical Learning: Data Mining, Inference, and Prediction. Second Edition, Springer.

37. Vermeulen P.T.M., Heemink A.W., and Stroet C.B.M.T. 2004. Reduced models for linear groundwater flow models using empirical orthogonal functions. Advances in Water Resources 27: 57-69.

38. van Doren J.F.M., Markovinovic R., and Jansen J.D. 2006. Reduced-order optimal control of water flooding using proper orthogonal decomposition. Computational Geosciences 10: 137-158.

39. Cardoso M.A., Durlofsky L.J., and Sarma P. 2009. Development and application of reduced-order modeling procedures for subsurface flow simulation. International Journal for Numerical Methods in Engineering 77(9): 1322-1350.

40. Rewienski M. and White J. 2003. A trajectory piecewise-linear approach to model order reduction and fast simulation of nonlinear circuits and micromachined devices. IEEE Transactions on Computer-Aided Design of Integrated Circuits and Systems 22(2): 155-170.

41. Cardoso M.A. and Durlofsky L.J. 2010. Linearized reduced-order models for subsurface flow simulation. Journal of Computational Physics 229(3): 681-700.

42. He J., Saetrom J., and Durlofsky L.J. 2011. Enhanced linearized reduced-order models for subsurface flow simulation. Journal of Computational Physics 230: 8313-8341.

43. Rousset M.A.H., Huang C.K., Klie H., and Durlofsky L.J. 2014. Reduced-order modeling for thermal recovery processes. Computational Geosciences 18: 401-415.

44. He J. and Durlofsky L.J. 2014. Reduced-order modeling for compositional simulation by use of trajectory piecewise linearization. SPE Journal 19: 858-872.

45. Jin, Z. 2015. Application of Reduced-Order Modeling for Geological Carbon Sequestration. MS thesis, Stanford University.

46. Carlberg K., Bou-Mosleh C., and Farhat C. 2011. Efficient non-linear model reduction via a least-squares Petrov-Galerkin projection and compressive tensor approximations. International Journal for Numerical Methods in Engineering 86(2): 155-181.

47. Zhou, Y. 2012 Parallel General-Purpose Reservoir Simulation with Coupled Reservoir Models and Multisegment Wells. PhD thesis, Stanford University.

48. Bonneville A. et al. 2013. Evaluating the suitability for CO_2 storage at the FutureGen 2.0 site, Morgan County, Illinois, USA. Energy Procedia, 37: 6125-6132.

49. He J., Sarma P., and Durlofsky L.J. 2013. Reduced-order flow modeling and geological parameterization for ensemble-based data assimilation. Computers & Geosciences 55: 54-69.

3. Uncertainty and Sensitivity Analysis Based Validation of Simplified Models

3.1 Introduction

The previous chapter described the development and validation of simplified physics based, statistical learning based and reduced order method based models for CO_2 geologic sequestration in stratified aquifer-caprock systems. One of the intended applications of such models is in the integrated system performance assessment of geologic CO_2 sequestration operations – especially if the analyses are carried out in a probabilistic framework to deal with model and parameter uncertainty. Therefore, another research goal of this project is ensure that these simplified models are also capable of reproducing the full spectrum of uncertainty and sensitivity analysis results from detailed numerical simulators. Specifically, it is important to verify that the cumulative distribution function (CDF) of outcomes from the detailed and simplified models are in reasonable agreement, and the importance ranking of key uncertain variables from both sources is similar. Such a "validation" step (in addition to the standard benchmarking using deterministic test cases as described in the previous chapter) would add to the credibility of systems model from a decision-maker's perspective.

In this chapter, an evaluation of the uncertainty and sensitivity analysis performance of the various types of simplified models developed in Sections 2.2 and 2.3 will be carried out in a Monte Carlo simulation framework. In what follows, the simulation cases and input parameters are described first, followed by the methodology for carrying out the validation. Next, the results of the analyses are presented, along with some concluding remarks.

3.2 Description of simulation cases and parameters

As described previously in Section 2.2.3, the basic model to be utilized is that of a single-well injecting supercritical CO_2 for 30 years into a 2-D radial-cylindrical bounded domain initially filled with brine. The model domain consists of a porous and permeable reservoir, overlain by a low-permeability caprock. The top of the caprock, the bottom of the reservoir and the lateral boundary are all assumed to be no-flow boundaries. The relevant model parameters are defined below in Table 3-1 for a reference case, as well as for "high" and "low" variants. In addition, the parameter ranges in Table 3-1 have also been transformed into probability distributions for Latin Hypercube Sampling, as shown in Table 3-2.

Table 3-1. Parameter values for the reference case and the two variants.

	Parameter	Description	Units	Reference value	Low Value	High Value	Comments
1	h_R	Thickness of reservoir	m	150	50	250	
2	h_{CR}	Thickness of caprock	m	150	100	200	
3	$k_{avg,R}$	Average horizontal	mD	46	12	220	

		permeability of reservoir					
	V_{DP}	Dykstra-Parson's coefficient	--	0.55	0.35	0.75	perfectly correlated with kavg,R
4	$k_{avg,CR}$	Average horizontal permeability of caprock	mD	0.02	0.002	0.2	
5	k_V/k_H	Anisotropy ratio	--	0.1	0.01	1	
6	q	CO2 Injection rate	MMT/yr	0.83	0.33	1.33	
	L	Outer radius of reservoir	km	10	5	7	perfectly correlated with q
7	ϕ_R	Porosity of reservoir	--	0.12	0.08	0.18	
8	ϕ_{CR}	Porosity of caprock	--	0.07	0.05	0.1	
9	I_k	Indicator for permeability layering	--	random	Increasing from top	Increasing from bottom	

Table 3-2. Input Distributions used with LHS Sampling

Input	Description	Distribution
h_R	Thickness of the reservoir	T(50,150,250)
h_{CR}	Thickness of the caprock	T(100,150,200)
μ_{lnk_R} V_{DP}	Log-mean reservoir permeability, Dykstra-Parson's coefficient (perfectly correlated)	$\mu_{lnk\_R} \sim$ T(2.45, 3.56, 4.67) $V_{DP} \sim$ T(0.35, 0.55, 0.75)
k_{CR}	Average caprock horizontal permeability	lnT(0.002,0.02,0.2)
k_V/k_H	Anisotropy ratio	lnT(0.01,0.1,1)

q	CO₂ injection rate	discrete with equal probability - {0.33, 0.83, 1.33}
φ_R	Porosity of the reservoir	T(0.08,0.12,0.18)
φ_{CR}	Porosity of the caprock	T(0.05,0.07,0.10)
I_k	Order of permeability layering	Discrete w/equal probability, $I_k \in$ {"random", " increasing", "decreasing"}

The following approach will be used for the uncertainty and sensitivity analysis.

- The performance metrics of choice are: (1) total storage efficiency, and (2) average reservoir pressure.
- Start with the 97-run Box-Behnken design simulations, fitted with a quadratic polynomial model. Consider this to be the "Model A". Also, utilize the 97-run maximin LHS design simulations, fitted with a kriging metamodel. Consider this to be the "Model B". See section 2.3.4 for details on these models.
- Next, utilize the simplified physics based models reported previously in Sections 2.2.5-2.2.7. Consider this to be "Model C".
- Create an LHS design with 10,000 samples based on Table 3-2.
- Compute the two performance metrics (step 1 above) at each of these sample points using Models A, B and C. Calculate the empirical CDF.
- Compare the 10,000 sample empirical CDF to the 97-sample empirical CDF.

3.3   Analysis Methodology

3.3.1   Statistical learning based models (Models A and B)

The initial assessment described in Section 2.3 provided information about which design/model combinations performed the best across three different responses from the GEM simulation. Of these, two were selected for the uncertainty analysis, based on both accuracy and robustness across the responses. These are the Box-Behnken design with quadratic regression (denoted Model 'A') and the maximin LHS design with kriging (denoted Model 'B'). Both of these designs were of size n = 97.

One measure of the quality of an approximation model is how well the range and distributions of estimated responses across the input space match the true distribution of responses. In this case, the true distribution of responses cannot be feasibly known, but a proxy for it is the empirical distribution produced by responses from the GEM simulation run over a small space-filling design. For this purpose, a 97-run LHS design was used to gather responses from the simulator that were evaluated at points in the input space that were completely independent of those used to fit Models 'A' and 'B'. Those responses were then used to construct an empirical CDF for the true response over the problem domain.

In order to generate the range and distribution of estimated responses over the input space, the Models 'A' and 'B' were evaluated at all locations in a 10,000-run LHS design. With such a large sample size, the

modeled responses across this design provide a good representation of the responses one might expect across all combinations of input parameter values.

The "closeness" of the true and estimated empirical distributions was measured using two different techniques. A common procedure for determining whether distributions match is the Kolmogorov-Smirnov (KS) test [1]. In this test, the null hypothesis H0 is that the distributions are the same, and the alternative is that they are different. The KS statistic is the largest gap between the CDFs. For this analysis, the p-value of the KS test was used to describe the closeness of the distributions. Larger p-values (up to a maximum of 1) indicate more similar distributions.

The second measure used to capture the closeness of the distributions is called "earthmover's distance"[2] (EMD). The concept here is that the two empirical distributions, represented as probability density functions (in, e.g., histogram form) can be thought of as mounds of earth. The earthmover's distance measures the least amount of work required to redistribute the earth in one distribution such that it matches the profile of the other distribution. In this case, a low value indicates similar distributions, while a large value indicates dissimilar distributions.

3.3.2   Simplified physics-based models (Model C)

Simplified physics based modeling runs use the simulation results from the LHS design runs (97 nos.) as the reference case for the Uncertainty Analysis task. A separate 10000 run sample LHS dataset is our test dataset. Model 'C' calculations estimate the final pressure using the predictive model for injectivity. CO$_2$ properties at evaluated at this final pressure and temperature which is then used to predict the plume extent followed by the average pressure buildup in the reservoir at the end of the CO$_2$ injection period. Inputs consist of the following known system parameters:

- Slope of CO$_2$ fractional flow curve, df_g/dS_g
- Initial pressure i.e. P_{init} (psi)
- Temperature, T (degree F)
- Formation brine salinity, Sal (fraction)
- CO$_2$ injection rate, q (tonnes per year)
- Time of injection, t (yr)
- Reservoir thickness, h_R (m)
- Reservoir average porosity, φ_R (fraction)
- Radial extent of reservoir, L (m)
- Reservoir permeability anisotropy ratio, $(k_v/k_h)_R$
- Total compressibility (pore + brine compressibility), $C_t = C_f + C_w$ (1/psi)
- Caprock thickness, h_{CR} (m)
- Caprock porosity, φ_{CR} (fraction)
- Array of values corresponding to layer permeability values in the system, [kR$_{layers}$] arranged from the top through the bottom layers.

Refer Section 2 for the discussion of the input sources of the above-mentioned parameters for use in the simplified predictive models.

The calculations steps in our MATLAB code for model "C" are as follows:

1. Calculate measures of heterogeneity from the permeability array input, thickness and porosity of each of the reservoir layers.

   1(a)   Mean reservoir permeability, k_R – calculated from the arithmetic mean of [kR_{layers}] in mD. This assumes all layers have equal thickness which is the case for our simulation runs.

   1(b)   Dykstra-Parsons co-efficient, V_{DP} – calculated from the mean of the log permeabilities i.e. μ_{lnk_R}. V_{DP} and μ_{lnk_R} are taken to be perfectly correlated inputs and we have μ_{lnk_R} = [2.45,3.56,4.67] corresponding to V_{DP} = [0.35,0.55,0.75].

   1(c)   Lorenz co-efficient, L_C – calculated while honoring the permeability layering/ arrangement from the bottom to top permeability layer in the reservoir.

$$L_C = 2\left\{\int_0^1 F_n dC_n - \frac{1}{2}\right\} \qquad \text{... (3.1)}$$

where cumulative flow capacity, $F_n = \frac{\sum_{i=1}^n k_{Ri}h_{Ri}}{\sum_{i=1}^N k_{Ri}h_{Ri}}$

and cumulative storage capacity, $C_n = \frac{\sum_{i=1}^n \phi_{Ri}h_{Ri}}{\sum_{i=1}^N \phi_{Ri}h_{Ri}}$

2. Determining final reservoir pressure P_f to calculate CO_2 properties more accurately

   2(a)   Calculate P_D using df_g/dS_g and V_{DP} in our simplified predictive model for dimensionless CO_2 injectivity.

$$P_D = 10.3 + 0.59\frac{df_g}{dS_g} + 3.41V_{DP} + 1.23\frac{df_g}{dS_g}V_{DP} - 0.342\left(\frac{df_g}{dS_g}\right)^2 - 8.89(V_{DP})^2 \qquad \text{... (3.2)}$$

   2(b)   Use this P_D to estimate the initial guess of the final pressure P_f at time t in field units.

$$J_{calc} = \frac{q\left(\frac{bbl}{day}\right)}{(P_f - P_{init})(\text{psi})} = \frac{k_R h_R \ (\text{mD.ft})}{141.2\mu_w(\text{cP})P_D} \qquad \text{... (3.3)}$$

With this initial guess value, solve for P_f such that

q/(P$_f$)/[P$_f$-P$_{init}$] matches {q/[P$_f$-P$_{init}$] = (2.pi.k$_R$.h$_R$)/(P$_D$.μ_w)}

3. Get q in bbl/day at time t using CO_2 properties at P_f and T.

4. Calculate Gravity number, N_g using CO_2 properties at P_f and T in SI units

$$N_g = \frac{k_R h_R (\text{m}^3)(\rho_w - \rho_{CO2})(\text{kg/m}^3) g h_R (\text{m}^2/\text{s}^2)(^{h_R}/_L)}{q \left(\frac{\text{m}^3}{\text{s}}\right) \mu_{CO2}(\text{kg/ms})(^{k_V}/_{k_H})} \qquad \text{... (3.4)}$$

where, $kV = (k_v/k_h)_R * k_R$

5. Maximum plume extent, R_{CO2} calculation using E_S:

   5(a)   Calculate total storage efficiency, E_S (%) from df_g/dS_g, VDP, L_C and N_g using the simplified predictive model:

$$E_S = 30.6862 + 0.4348\frac{df_g}{dS_g} + 29.2359L_C - 22.018V_{DP} - 11.2445N_g + 4.5962\frac{df_g}{dS_g}V_{DP}$$
$$- 25.2141L_C V_{DP} - 0.6917\left(\frac{df_g}{dS_g}\right)^2 + 6.1074(N_g)^2 \qquad \text{... (3.5)}$$

   5(b)   Calculate m3 free phase CO_2 present in reservoir at time t i.e. Q_{cum} using an average factor of 0.8 used to account for the free phase CO_2 from the total CO_2 present. This factor is determined for our calculations as the representative average value for the uncertainty analysis exercise from simulation runs (that use Henry's law).

   5(c)   Calculate CO_2 plume extent in meters at time, t, in SI units

$$R_{CO2} = \sqrt{\frac{100Q_{cum}(\text{m}^3)}{\pi\phi_R(\text{fraction})h_R(\text{m})E_S(\%)}} \qquad \text{... (3.6)}$$

6. Average reservoir pressure buildup, $\Delta P_{R,avg}$ calculation using simplified model for dimensionless average reservoir pressure buildup P_{D1}

   6(a)   Calculate f

$$f = 0.003(\frac{L}{R_{CO2}})^2 + 0.774 \qquad \text{... (3.7)}$$

   6(b)   Calculate f_{sc}

$$f_{SC} = \frac{\phi_R h_R}{(\phi_R h_R + \phi_R h_R)} \qquad \text{... (3.8)}$$

   6(c)   Calculate combined factor, ft

$$f_t = f f_{SC} \qquad \text{... (3.9)}$$

   6(d)   Calculate dimensionless time, t_{DA1}, in field units

$$t_{DA1} = \frac{0.0002637 k_R(\text{mD}) t(\text{hr})}{\phi_R(\text{fraction}) \mu_w(\text{cP}) C_t(\frac{1}{\text{psi}}) \pi L^2(\text{ft}^2)} \quad \text{... (3.10)}$$

6(e)   Calculate dimensionless average reservoir pressure buildup, P_{D1}

$$P_{D1} = 2\pi f_t t_{DA1} \quad \text{... (3.11)}$$

6(f)   Calculate average reservoir pressure buildup, $\Delta P_{R,avg}$, in psi

$$\Delta P_{Ravg} = \frac{141.2 q_f(\frac{\text{bbl}}{\text{day}}) \mu_w(\text{cP}) P_{D1}}{k_R(\text{mD}) h_R(\text{ft})} \quad \text{... (3.12)}$$

7. Treatment of outliers to eliminate nonphysical predictions: Outliers are those that satisfy the following criteria:

- Gravity number greater than the threshold value of 2 i.e. Ng> Ng threshold of 2

- h_R/h_{CR} cases that have higher injection in thin reservoirs i.e. h_R/h_{CR} <=0.5 and q>=1.33 MT/yr

8. Generate the empirical Cumulative Distribution Functions (CDFs) for R_{CO2} and $\Delta P_{R,avg}$ from both the reference and test datasets.

9. Compare CDFs of both LHS datasets with the KS-test statistic and the EMD statistic.

3.4   Results – Simplified Physics Based Models

We consider the plume radius and the average reservoir pressure buildup at the end of CO$_2$ injection period to be our performance metrics of interest for the uncertainty analysis exercise. In the case of Models 'A' and 'B', the response is average reservoir pressure after 30 years, which is identical to the pressure buildup with a shift of a constant, and does not affect the shape of the distribution. For each of our three chosen models, the cumulative distribution function (CDF) generated from the simulation responses for the 97-run reference LHS design is compared with the cumulative distribution function generated from the model prediction across the 10,000-run LHS design. The performance of each of the models is sequentially discussed and compared.

Model 'C' is successfully validated by testing the code for both the Task 2 training dataset followed by the 97-run reference LHS dataset. Fig. 3-1 gives the resulting cross-plots of the model predictions for the LHS reference dataset versus the corresponding detailed simulator results for the plume radius and the average reservoir pressure buildup.
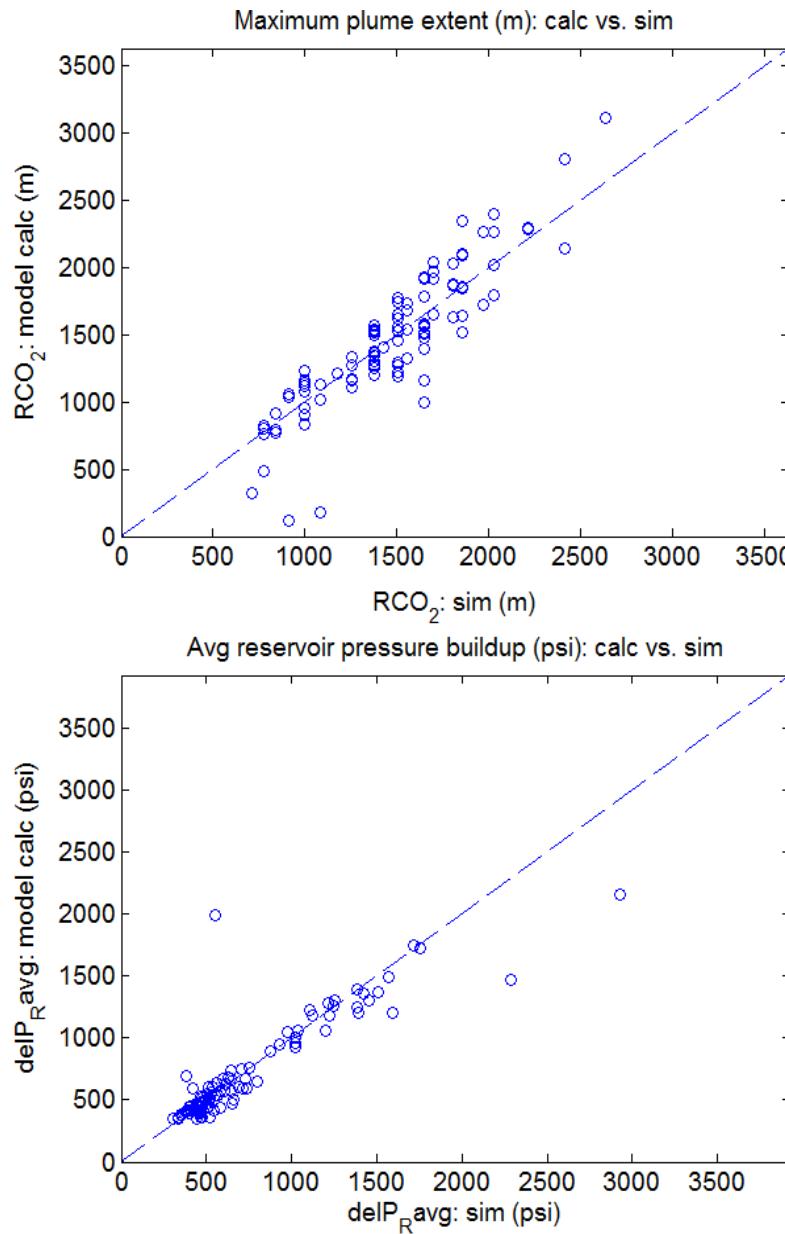
Fig. 3-1. Scatter plot showing the model 'C' predictions versus the detailed numerical simulator results for plume radius and average reservoir pressure buildup with the 97-run reference LHS dataset

The CDF generated from the simulation results for the 97-run reference LHS dataset represent the simulation 'reference curve' for our uncertainty analysis. The black CDF curve in the following figures is this reference CDF curve. The red CDF curve in each plot is the cumulative distribution function generated from the model prediction across the 10,000 run LHS 'test' design for the performance metric indicated in the title of each plot. The CDF comparison plot for plume extent and average reservoir pressure buildup from Model 'C' is shown in Fig. 3-2.

Empirical CDF: LHS10k (RCO2)
KS 0.0030, EMD 0.1094

Empirical CDF: LHS10k (delPRavg)
KS 0.1199, EMD 0.0319
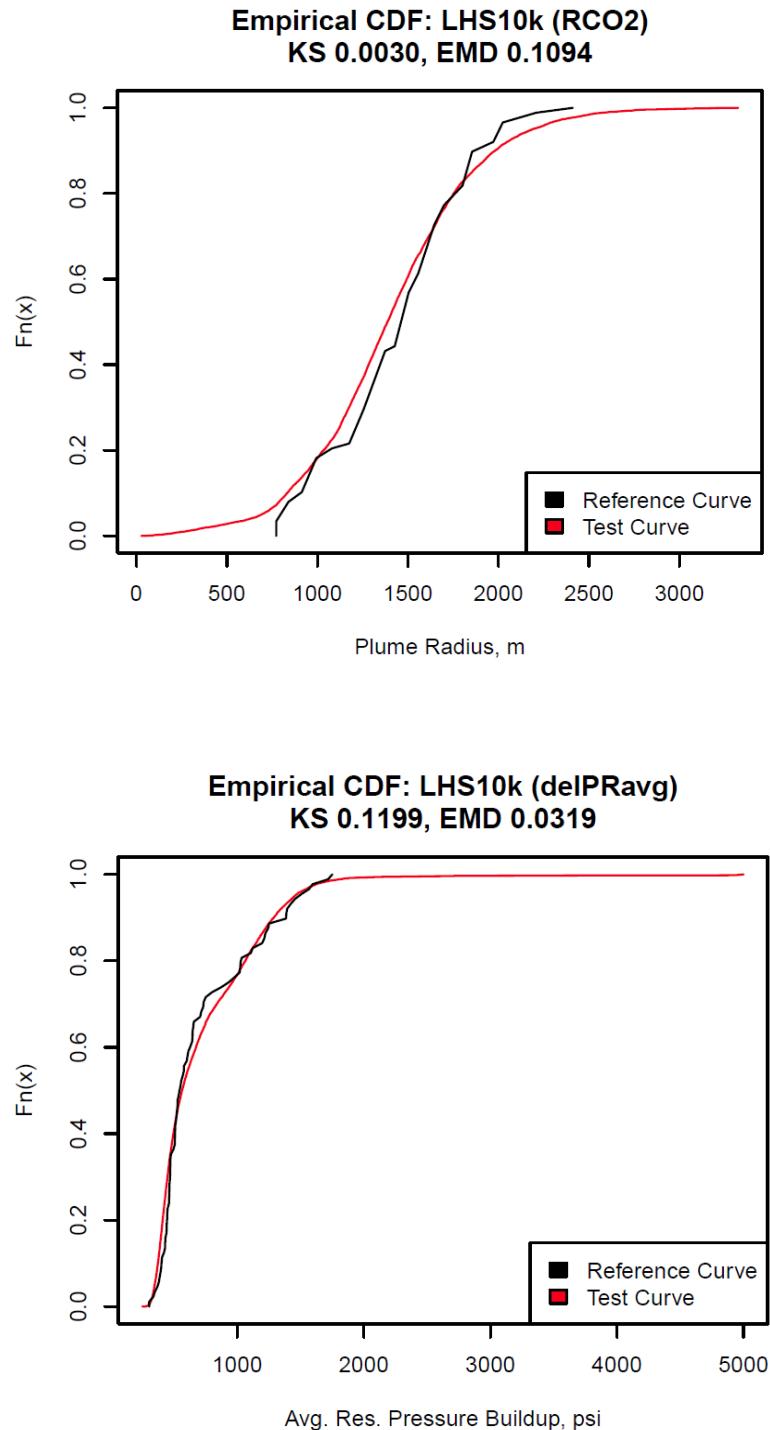
Fig. 3-2. Comparison plot of CDF of 97-sample 'reference' LHS simulation results and 10,000 sample 'test' model predictions. (a) plume radius (m); (b) average reservoir pressure buildup (psi).

We observe 7% of the 'test' dataset produce outliers with nonphysical predictions of the total storage efficiency or erroneous pressure buildup when computed using the simplified physics-based models. Certain combinations of input parameter values sampled using the LHS design sometimes leads to such outlier cases cause the tail effect in the model test curves (red curves) in Fig. 3-2. Cases such as large injection in thin reservoirs result in big difference between the simulation and prediction results.

We analyze the input parameters in each of our datasets to determine the relationship between nonphysical model predictions of total storage efficiency and input parameter limits. Fig. 3-3 is a scatterplot representation illustrating the effect of L_C, V_{DP} and N_g values on E_S predictions.
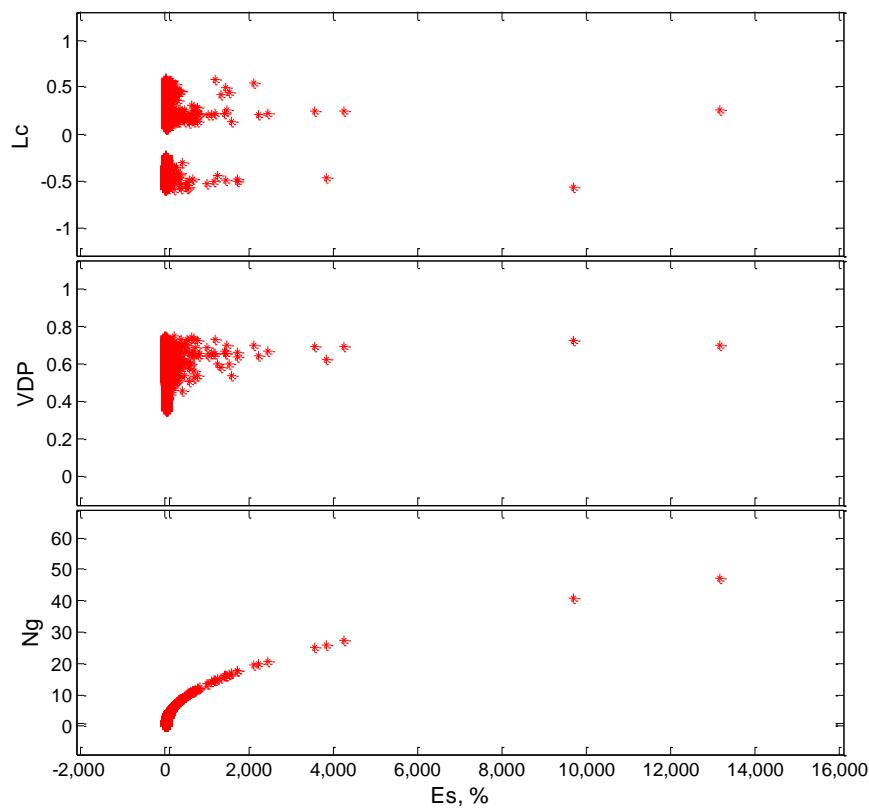
Fig. 3-3. Scatter plots showing Es model predictions getting to nonphysical values with increasing gravity number cases for the 'test' LHS design.

Fig. 3-3 shows how increasing Gravity number cases lead to nonphysical predictions of total storage efficiency (i.e. $E_S > 100\%$). The range of Gravity numbers is much higher in the LHS datasets compared to the range of Gravity numbers sampled in our Task 2 training dataset as shown in Fig. 3-4. Hence predictions using model 'C' for these higher Gravity number cases in the LHS datasets result in much higher E_S values and consequently much lower plume extents compared to the detailed simulation results. A threshold gravity number of 2 honors the range of our output performance metrics effectively and has been used to eliminate outlier cases in our analysis.
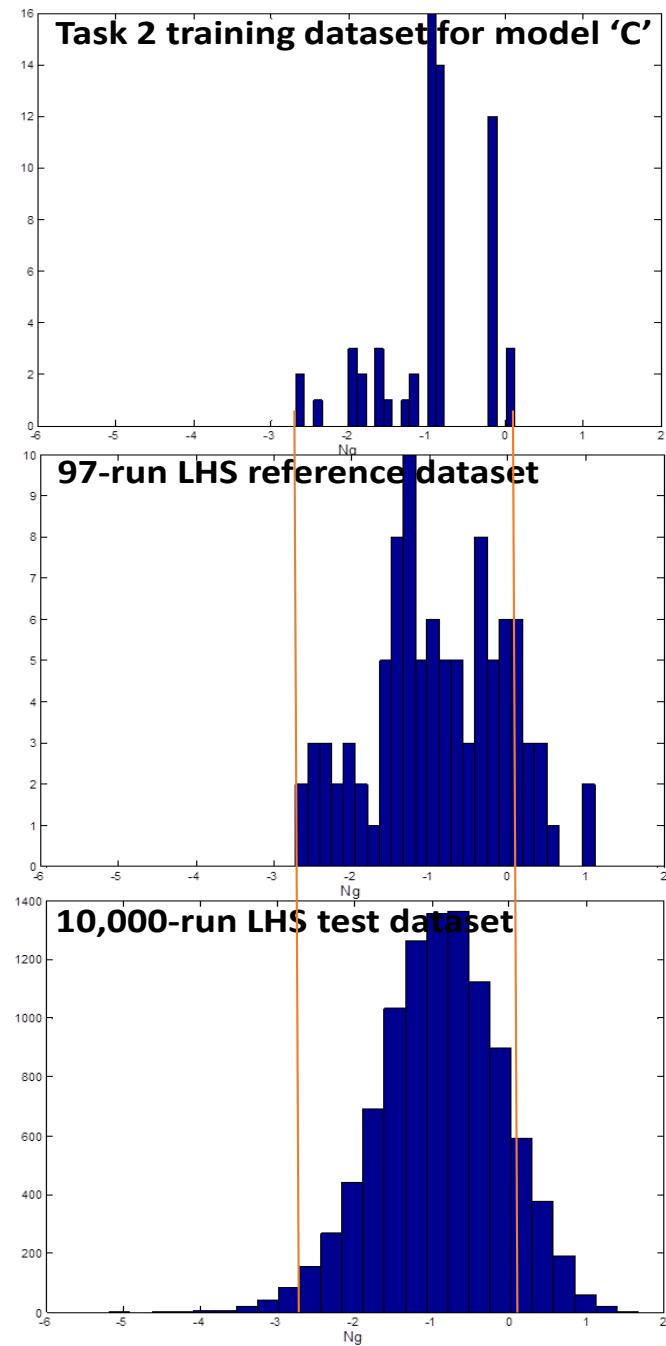
Fig. 3-4. Comparison of histograms of log(Gravity number) showing the increasing range of values as we move from the Task 2 training dataset to the 97-run LHS reference dataset and the 10000-run LHS test dataset.

Hence, we treat the model results from our LHS datasets to conform to the below-mentioned parameter limits and hence eliminate outlier cases:

- Applying threshold gravity number of 2 as the cut-off (i.e., $N_{g,max} = 2$) to treat nonphysical predictions of total storage efficiency.
- Applying cut-offs $h_R/h_{CR} < 0.5$ and $q \geq 1.33$ MT/yr cases to eliminate average reservoir pressure buildup outliers.

The elimination of outliers from the predictions of the total storage efficiency and dimensionless average reservoir pressure buildup models result in the empirical CDFs shown in Fig. 3-5.

The consequent model 'C' predictions of maximum plume extent and the average reservoir pressure buildup result in the modified empirical CDFs shown in Fig. 3-6.

Hence we verify that the CDF of outcomes from the simplified physics based models generated after treatment for outliers are in reasonable agreement to the simulation results for the full spectrum of sensitivity analysis results.
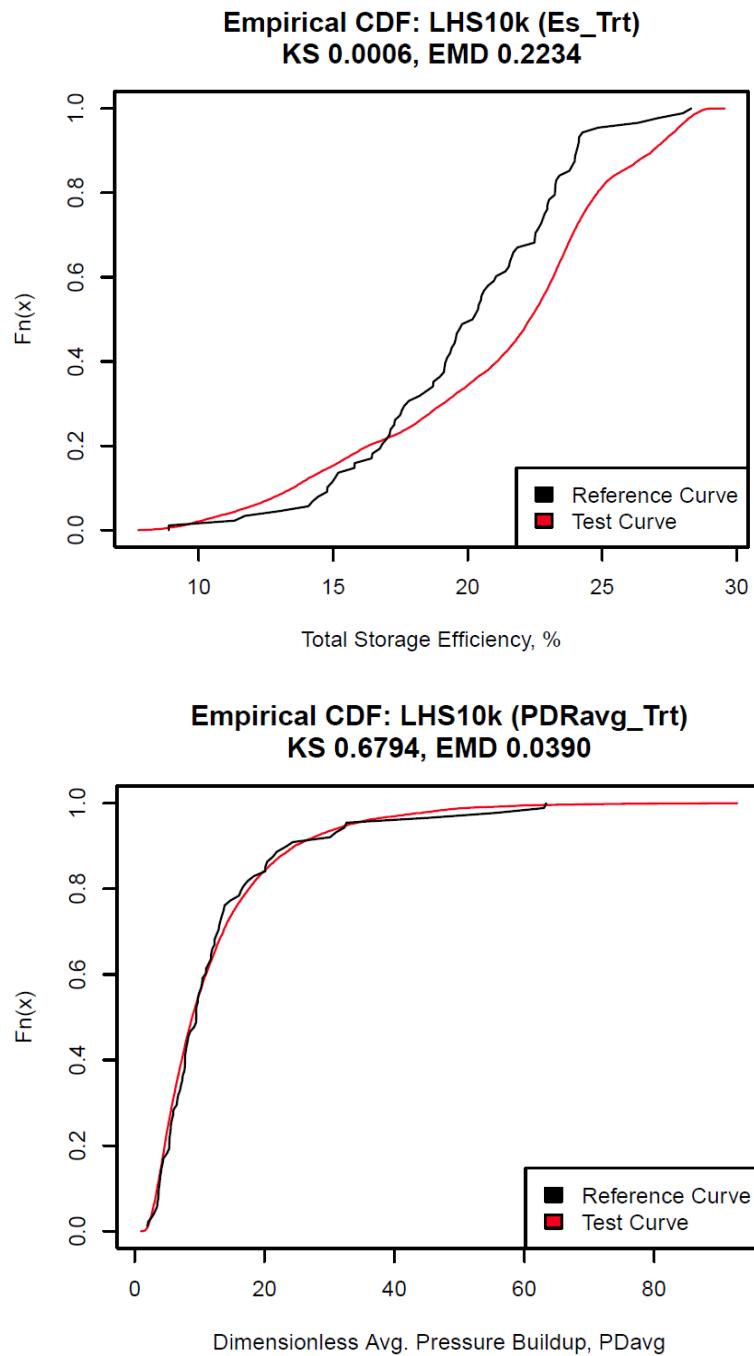
Fig. 3-5. Comparison plot of CDF of 97-sample 'reference' LHS simulation results and 10,000 sample 'test' model predictions after treatment of outliers. Performance metrics in the panels consist of: top – total storage efficiency (%) and bottom – dimensionless average reservoir pressure buildup.
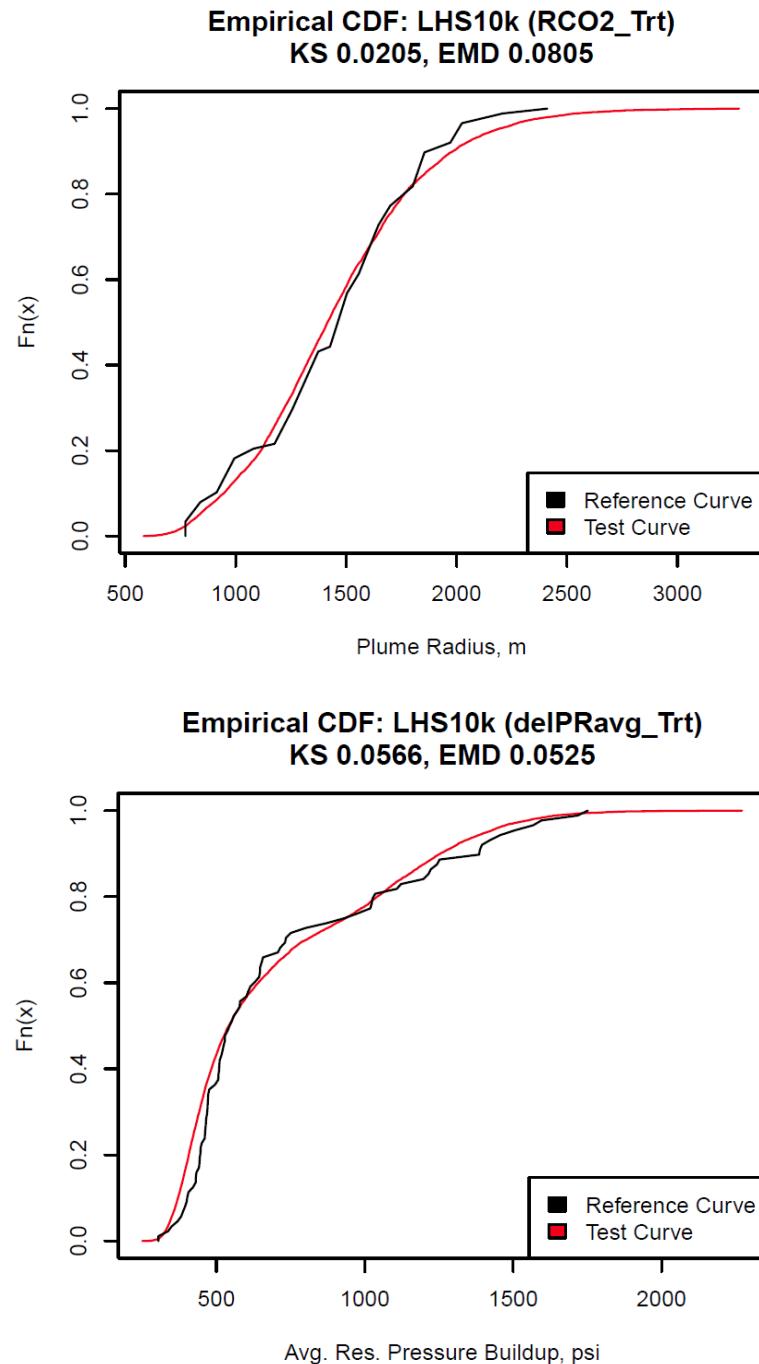
Fig. 3-6. Comparison plot of CDF of 97-sample 'reference' LHS simulation results and 10,000 sample 'test' model predictions after treatment of outliers. Performance metrics in the panels consist of: top – maximum plume extent (m) and bottom – average reservoir pressure buildup (psi). Plot titles also indicate the corresponding KS-test and EMD statistics.

3.5 Results – statistical learning based models

To perform the comparison between the true and estimated response distributions for the statistical learning based models, both models were evaluated at each of the 10,000 runs in the LHS test design. The CDF of those responses was then compared to the true CDF, which was taken to be the GEM simulation response over the independent 97-run LHS design. Fig. 3-7 shows the comparisons for Model 'A' (Box-Behnken design with quadratic metamodel), and Fig. 3-8 shows the comparisons for Model 'B' (Maximin LHS design with Kriging metamodel). Both models show general agreement with the response for the reference model for both responses.
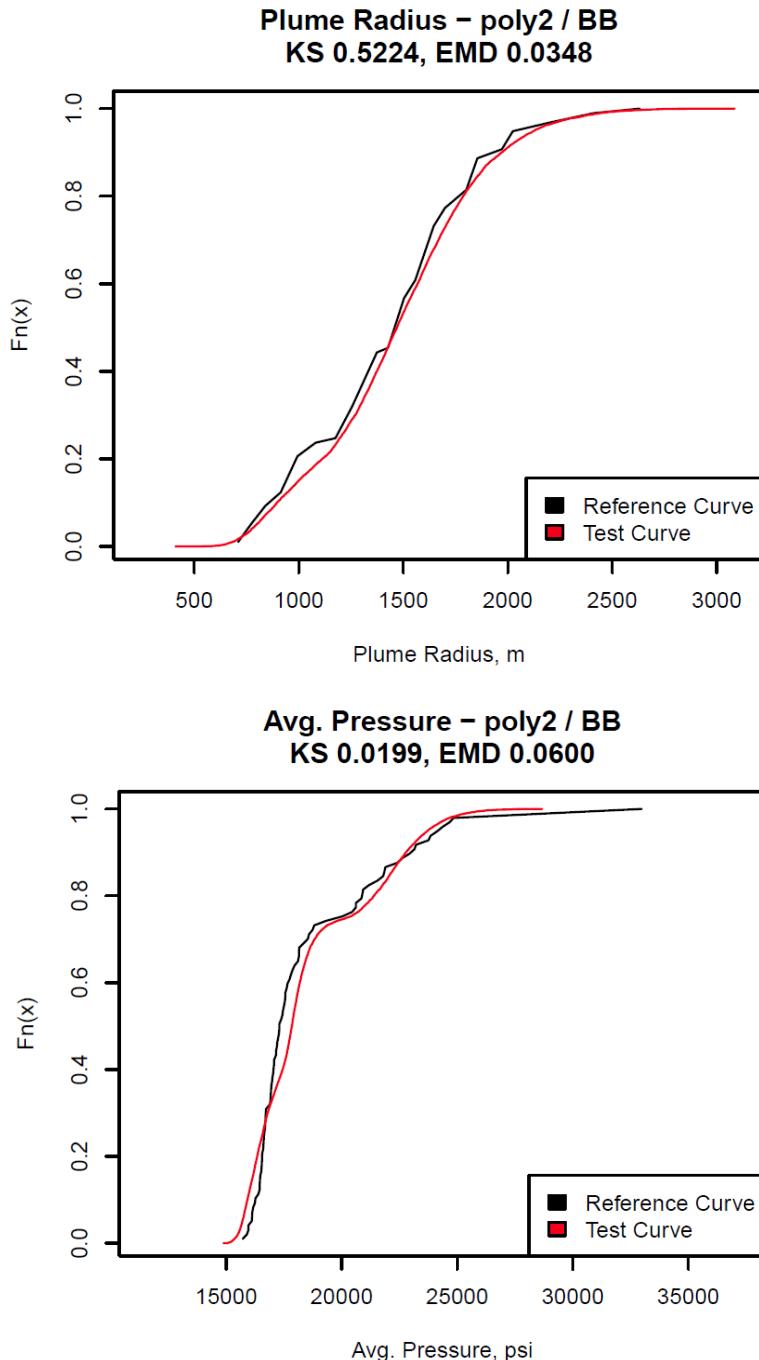
Fig. 3-7. Comparison plots of CDFs for the 97-sample 'reference' LHS simulation results vs. the 10,000 sample 'test' model predictions for Model 'A' (Box-Behnken design with quadratic metamodel). Performance metrics in the panels consist of: top – maximum plume extent (m) and bottom – average reservoir pressure (psi). Plot titles also indicate the corresponding KS-test and EMD statistics.
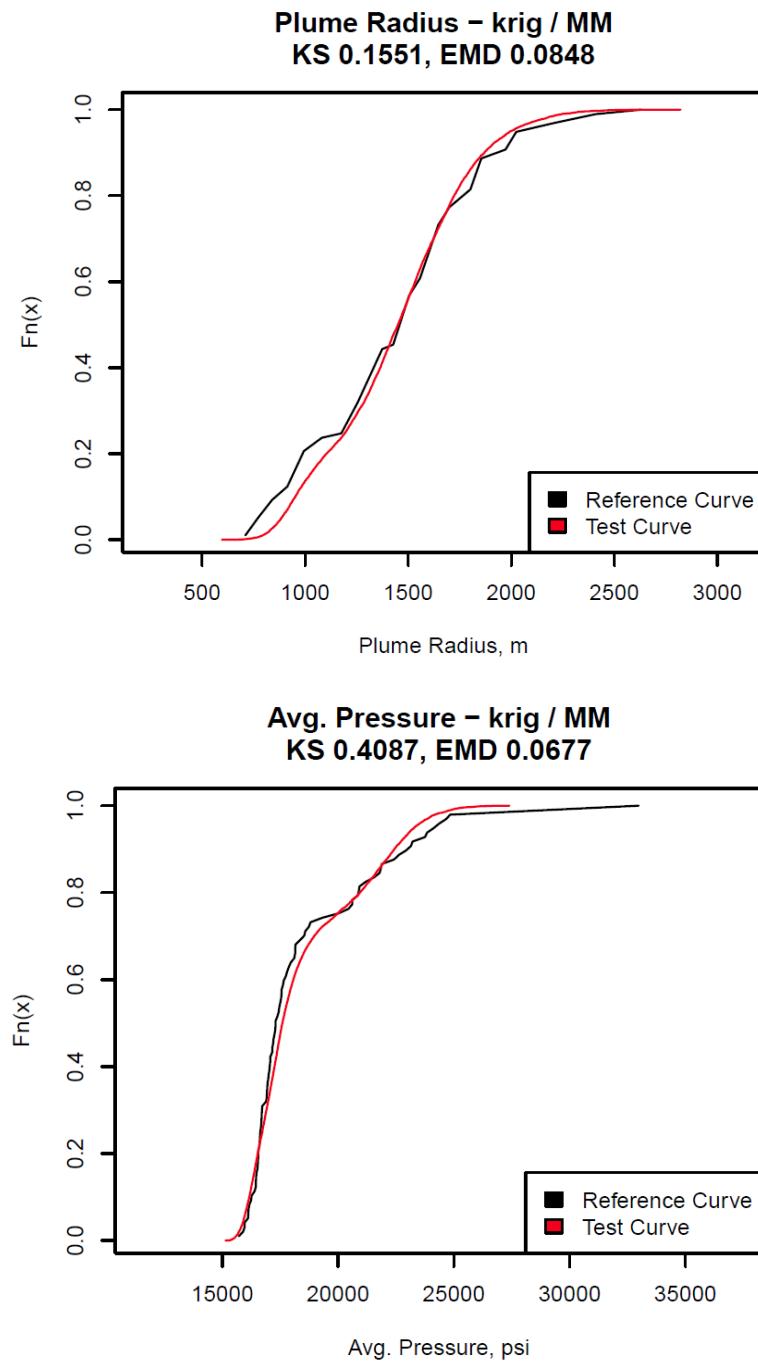
Fig. 3-8. Comparison plots of CDFs for the 97-sample 'reference' LHS simulation results vs. the 10,000 sample 'test' model predictions for Model 'B' (Maximin LHS design with kriging metamodel). Performance metrics in the panels consist of: top – maximum plume extent (m) and bottom – average reservoir pressure (psi). Plot titles also indicate the corresponding KS-test and EMD statistics.

3.6   Comparison of Models

Our objective in this phase of the research was to validate our simplified physics and statistical learning based models for plume and pressure propagation in semi-confined aquifer systems in a probabilistic setting. Additionally, our goal was to establish confidence-levels on their credibility and rank their performance against each other. We generated and verified that the CDF of outcomes from the simplified physics models are in reasonable agreement to the simulation results for the full spectrum of sensitivity analysis results.

The three chosen modeling approaches (i.e., the two statistical learning based models, Model A and Model B, and the simplified-physics based model, Model C) can be compared using the KS-test statistic and the EMD statistic to rank their relative performance.

Table 3-3: Model Performance Comparison

Performance metric	Model 'A'	Model 'B'	Model 'C'
Plume extent			
Earth Mover's distance (EMD) statistic	0.035	0.085	0.081
KS-test statistic	0.522	0.155	0.021
Average reservoir pressure buildup			
Earth Mover's distance (EMD) statistic	0.060	0.068	0.053
KS-test statistic	0.020	0.409	0.057

We observe that while all models agree reasonably with the simulation results, the best model fits for our performance metrics turn out to be the statistical learning based models. Model 'A' performs best for the plume extent while model 'B' performance best for the average reservoir pressure buildup. The simplified physics based models have been trained using a smaller subset of the input parameter values which do not possibly cover the entire input parameter space compared to the statistical models developed using space-filling designs. This could possibly explain the tail seen in the Model 'C' predictions in Fig. 3-2.

References

[1] Myles Hollander and Douglas A. Wolfe (1999). Nonparametric Statistical Methods. 2nd Edition, John Wiley & Sons, Inc.: New York.

[2] Yossi Rubner; Carlo Tomasi; Leonidas J. Guibas (1998). "A Metric for Distributions with Applications to Image Databases". Proceedings ICCV 1998: 59–66.

4. Conclusions and Recommendations

4.1 Conclusions

Key conclusions from this research project can be summarized as follows:

- We developed and validated simplified predictive models for dimensionless pressure buildup (i.e., well injectivity and average reservoir pressure) and total storage efficiency (i.e., plume radius), in terms of key underlying parameters combined into dimensionless groups, based on insights from full-physics simulations,

- We compared the performance of a traditional experimental design based surrogate modeling strategy (i.e., Box-Behnken design combined with quadratic model) to a sampling-based design and metamodeling strategy (i.e., maximin Latin Hypercube sampling combined with multidimensional kriging) using a k-fold cross-validation strategy,

- We demonstrated the applicability of the POD-TPWL approach to reduced-order modeling for CO_2-brine systems – with vertical and horizontal wells, under BHP and rate control, as well for geologic perturbations – as a computationally-efficient alternative to full-order simulations showing speedups upto a factor of ~370, and

- We validated the simplified physics and statistical learning based approaches using an uncertainty analysis framework wherein CDF of outcomes from the simplified models were found to be in reasonable agreement with detailed numerical simulation results after eliminating non-physical outliers.

4.2 Recommendations for Future Work

4.2.1 Simplified physics based models

- The range of conditions used to develop the simplified-physics based models (e.g., Table 2-1) should be expanded, particularly with respect to the relative permeability variants.

- Alternatives to df_g/dS_g (slope of gas fractional flow curve) – as a "bulk" representation of relative permeability relationships – should be explored in greater detail.

- The impact of time-dependence on CO_2 plume extent models should be studied.

4.2.2 Statistical learning based models

- The issue of appropriate sample size of LHS simulations should be further studied.

- Applicability and efficacy of metamodels to capture time-dependent output behavior (as opposed to fitting the output at only selected points in time) should be studied.

- Better screening-level designs should be investigated.

- Robust variable importance ranking methods that do not require additional simulations beyond the primary experimental design should be explored.

4.2.3 Reduced-order method based models

- Improved formulations for constraint reduction (see section 2.4.2) should be studied.

- Further testing and assessment of the approach for handling geological perturbations (section 2.4.4c) in POD-TPWL should be investigated.

- Late-time deviations between full-order simulations and POD-TPWL for rate-control wells (section 2.4.4b) should be further studied.

- The applicability of POD-TPWL in a multi-well setting (i.e., network of injection wells) should be explored.

4.2.4 Uncertainty and sensitivity analysis based validation

- Automated methods of ensuring consistency between the sample space of the original simplified models and that used for probabilistic applications (and the elimination of non-physical parameter combinations) should be investigated.

- Additional schemes of comparing two different CDFs should be applied.

- Importance ranking from simplified and detailed models should be compared, in additional to comparing the similarity of CDFs.

- The uncertainty and sensitivity analysis based validation framework should also be applied for reduced-order method based models.

Acknowledgments

Appendix

Topical Report Excerpts

SIMPLIFIED PREDICTIVE MODELS FOR CO₂ SEQUESTRATION PERFORMANCE ASSESSMENT

RESEARCH TOPICAL REPORT ON TASK #2 SIMPLIFIED PHYSICS BASED MODELS

Reporting Period: July 1, 2014 through September 30, 2014

Principal Investigator: Dr. Srikanta Mishra
mishras@battelle.org 614-424-5712
Principal Authors: Priya Ravi Ganesh and Srikanta Mishra

Date Report Issued: October 2014

Submitting Organization:

Battelle Memorial Institute
505 King Avenue
Columbus, OH 43201
DUNS Number: 00 790 1598

Abstract

We present a simplified-physics based approach, where only the most important physical processes are modeled, to develop and validate simplified predictive models of CO_2 sequestration in deep saline formation. The system of interest is a single vertical well injecting supercritical CO_2 into a 2-D layered reservoir-caprock system with variable layer permeabilities. We use a set of well-designed full-physics compositional simulations to understand key processes and parameters affecting pressure propagation and buoyant plume migration. Based on these simulations, we have developed correlations for dimensionless injectivity as a function of the slope of fractional-flow curve, variance of layer permeability values, and the nature of vertical permeability arrangement. The same variables, along with a modified gravity number, can be used to develop a correlation for the total storage efficiency within the CO_2 plume footprint. Similar correlations are also developed to predict the average pressure within the injection reservoir, and the pressure buildup within the caprock.

Table of Contents

List of Appendices

Appendix I: Compilation of Figures and Data Tables

Appendix II: Similarity Solutions for Multiphase Flow in Inhomogeneous Layered Systems for CO₂ Sequestration

List of Figures

List of Tables

Executive Summary

The objective of this research project is to develop and validate a portfolio of simplified modeling approaches for CO_2 sequestration in deep saline formations – based on simplified physics, statistical learning, and/or mathematical approximations – for predicting: (a) injection well and formation pressure buildup, (b) lateral and vertical CO_2 plume migration, and (c) brine displacement to overlying formations and the far-field. Such computationally-efficient alternatives to conventional numerical simulators can be valuable assets during preliminary CO_2 injection project screening, serve as a key element of probabilistic system assessment modeling tools, and assist regulators in quickly evaluating geological storage projects. The project team includes Battelle and Stanford University. Support for the project is provided by U.S. DOE National Energy Technology Laboratory and the Ohio Development Service Agency Office of Coal Development (ODSA).

Over the last decade, the development and demonstration of geologic sequestration technologies to mitigate greenhouse gas emissions has been an area of active research. Geologic sequestration of CO_2 in deep saline formations has been recognized for its immense potential for long-term storage of captured CO_2. To ensure safe and effective deployment of this technology, it is crucial for us to understand the nature of pressure and plume propagation as injected CO_2 displaces the native reservoir fluids. Detailed numerical simulation of such processes generally requires extensive reservoir characterization data and computational burden. In this context, validated simplified models can be valuable as they have minimal data and computational requirements in comparison. Simplified models that are based on the most relevant physical processes and validated against full-physics simulators are thus being sought after as efficient and useful alternatives for rapid screening and evaluation of CO_2 sequestration projects.

This topical results presents results from Task2 of the research project. Our research objective is to develop and validate simplified physics based models for CO_2 sequestration in deep saline formations based on insights from a set of well-designed full-physics compositional simulations of this system. The study involves an extensive parameter space covering different reservoir and cap rock properties. We investigate the sensitivity of system behavior for high and low variants from a reference case for various reservoir and caprock properties and systematically seek to quantify their effect on each performance metric.

Our computational model consists of a single vertical well radially injecting supercritical CO_2 in the middle of a 2-D layered reservoir overlain by a caprock. We add relevant buoyancy and heterogeneity effects to the system considerations in the simplified 1-D 3-region model of Oruganti and Mishra (2013) and Burton et al. (2008). Simulations are run for an injection period of 30 years to observe CO_2 displacement characteristics in a closed system – as would be the case in a network of injection wells. The independent variables of interest are thickness and porosity of reservoir and caprock, reservoir permeability heterogeneity, permeability and capillary pressure of the caprock, and CO_2 injection rate. Reservoir heterogeneity is varied by controlling the permeability of the reservoir, permeability anisotropy ratio (ratio of vertical to horizontal permeability) in the reservoir, spatial arrangement of the heterogeneous reservoir permeability layers, and relative permeability curves for the reservoir.

The maximum plume extent at the end of CO_2 injection is affected by the efficiency of the two-phase (CO_2-brine) displacement process – this total storage efficiency, E_S, being a product of: (a) volumetric sweep efficiency i.e. fraction of total pore volume contacted by CO_2, and (b) displacement efficiency within the pore volume contacted by CO_2. We establish a relationship for maximum plume extent at the end of injection as a function of the amount of CO_2 injected and the storavitity (porosity-thickness product) of the reservoir, for a given total storage efficiency. The most important terms in the simplified model for total storage efficiency involve the relative permeability model followed by the reservoir heterogeneity.

CO_2 injectivity, which is the ratio of amount of CO_2 injected to the corresponding pressure buildup, is a critical performance metric to determine operational constraints of pressure buildup or injection rate for allowable injected volume of CO_2 or operating pressure constraints respectively. We consistently observe from the sensitivity analyses that our system response to CO_2 injection is such that the pressure at the injection well quickly jumps to a quasi-steady value and remains relatively stable thereafter during the early transient period before boundary effects come into play. This pressure jump can be converted into a dimensionless pressure buildup, P_D, which includes the effects of reservoir permeability-thickness, CO_2 injection rate and brine viscosity, and helps us effectively capture the injectivity index of the well

The pressure buildup at the mid-point of the reservoir is observed to be affected primarily by the permeability-thickness product of the reservoir, the CO_2 injection rate, and the relative permeability model for the reservoir. When expressed in terms of the dimensionless variable P_D, we determine the dimensionless pressure buildup at the CO_2 injector well to be a function of the slope of the fractional flow curve (df_g/dS_g) and the Dykstra-Parson's coefficient (V_{DP}). Thus, using a steady-state version of Darcy's law and dominant parameter groups identified from the sensitivity analysis exercise with full-physics compositional simulations, we develop a multivariate linear regression model to determine P_D, and hence, the injectivity index. This predictive model is successfully validated to check for robustness of fit.

We also evaluate the average pressure behavior in the reservoir for a given amount of CO_2 injected into closed and semi-closed saline formations. For closed reservoirs, the effectiveness of two-phase flow in a given reservoir depends on an 'ƒ' factor (which is a function of the relative permeability) and is correlated to the square of the ratio of the reservoir radius to the plume radius at the end of injection. For semi-closed formations when an overlying caprock is present, this 'ƒ' factor is modified to account for the relative storage capacity of the rock i.e. ratio of reservoir storavitity to the total system storativity.

Finally, the effect of the overlying cap rock properties – mainly thickness and permeability, were investigated for their effect on the pressure buildup in the system. The ratio of the pressure buildup in the cap rock to that in a given reservoir at the end of injection was determined to be a function of the ratios of the thickness and permeability of cap rock and the reservoir.

Thus, using the basic physical processes involved, these simplified physics models can be used to reasonably predict the plume extent in the reservoir and pressure propagation in both the reservoir and the cap rock resulting from the injection of a given amount of CO_2.

SIMPLIFIED PREDICTIVE MODELS FOR CO$_2$ SEQUESTRATION PERFORMANCE ASSESSMENT

RESEARCH TOPICAL REPORT ON TASK #3
STATISTICAL LEARNING BASED MODELS

Reporting Period: July 1, 2014 through September 30, 2014

Principal Investigator: Dr. Srikanta Mishra
mishras@battelle.org 614-424-5712
Principal Authors: Jared Schuetter and Srikanta Mishra

Date Report Issued: October 2014

Submitting Organization:

Battelle Memorial Institute
505 King Avenue
Columbus, OH 43201
DUNS Number: 00 790 1598

Abstract

We compare two approaches for building a statistical proxy model (metamodel) for CO_2 geologic sequestration from the results of full-physics compositional simulations. The first approach involves a classical Box-Behnken or Augmented Pairs experimental design with a quadratic polynomial response surface. The second approach used a space-filling maxmin Latin Hypercube sampling or maximum entropy design with the choice of five different meta-modeling techniques: quadratic polynomial, kriging with constant and quadratic trend terms, multivariate adaptive regression spline (MARS) and additivity and variance stabilization (AVAS). Simulations results for CO_2 injection into a reservoir-caprock system with 9 design variables (and 97 samples) were used to generate the data for developing the proxy models. The fitted models were validated with using an independent data set and a cross-validation approach for three different performance metrics: total storage efficiency, CO_2 plume radius and average reservoir pressure. The Box-Behnken–quadratic polynomial metamodel performed the best, followed closely by the maximin LHS–kriging metamodel.

Table of Contents

List of Figures

List of Tables

Executive Summary

The objective of this research project is to develop and validate a portfolio of simplified modeling approaches for CO_2 sequestration in deep saline formations – based on simplified physics, statistical learning, and/or mathematical approximations – for predicting: (a) injection well and formation pressure buildup, (b) lateral and vertical CO_2 plume migration, and (c) brine displacement to overlying formations and the far-field. Such computationally-efficient alternatives to conventional numerical simulators can be valuable assets during preliminary CO_2 injection project screening, serve as a key element of probabilistic system assessment modeling tools, and assist regulators in quickly evaluating geological storage projects. The project team includes Battelle and Stanford University. Support for the project is provided by U.S. DOE National Energy Technology Laboratory and the Ohio Development Service Agency Office of Coal Development (ODSA).

This topical report presents results from Task 3 of the research, which focuses on statistical learning based models, with the objective of identifying and comparing several different ways of creating such predictive models. These are commonly called "proxy models" or "metamodels" in the geoscience literature. In applications related to subsurface flow, response variables of interest are often simulated with full physics mathematical models that are based on a large number of predictor variables. When a deep understanding of the relationship between the predictors and response is required, e.g., for optimization, many runs of the predictors at different combinations of settings may be necessary. Due to time and cost, running such a model for a large number of runs may not be feasible. The idea of a proxy model is to first acquire a small number of simulation runs at prescribed combinations of predictors, called a design matrix. These combinations are specially chosen to be representative of all possible predictor settings, called the input space. The runs are also chosen to allow estimation of large scale effects in the response. Using the observed runs, a statistical model is then developed. This model describes a specific mathematical relationship between the predictor variables and the response.

A good metamodel needs to have two characteristics. First, it must provide an accurate approximation of the full physics simulation. That is, for any combination of predictor settings, the metamodel should predict a value of the response that is close to the value one would get by running the full simulation at the same settings. Second, the metamodel must run orders of magnitude faster than the full physics simulation. If these two requirements are met, then the metamodel may be used as a proxy for the full physics simulation, and since it can produce responses quickly, it can be used to explore the input space for optimal predictor combinations.

After conducting a survey of geoscience literature, several designs and models were selected for the comparison study. Regarding designs, both experimental and sampling design approaches were considered. From the former group, Box-Behnken (BB) and augmented pairs (AP) designs were selected. BB designs are the industry standard, and AP is a competitor of the BB that uses fewer runs. From the latter group, maximum entropy (ME) and maximin Latin hypercube sampling (LHS) designs were selected. LHS designs are also popular in the geoscience literature, and ME designs are a leading competitor.

Regarding modeling techniques, five different approaches were considered. These include quadratic polynomial regression, which is common in oil and gas applications; kriging, which is a popular choice often used with LHS designs; MARS, which is another method often cited in the literature; and AVAS, which is a non-parametric modeling option. In addition, a version of quadratic modeling that uses LASSO variable selection was also considered as a more refined alternative to traditional quadratic regression modeling.

All 20 combinations of designs and models were used to predict each of three responses in a 9-input full-physics simulation of CO_2 injection into a closed reservoir using the compositional simulator, GEM. The performance of each metamodel was evaluated by fitting to this data set using three criteria: root mean squared error (RMSE), scaled RMSE, and pseudo-R^2. Evaluation was performed both for 5-fold cross-validated predictions on the training set as well as predictions on an independent test set.

In this latter case, the traditional approach of a BB design with a quadratic regression model came out as the top performer in terms of general performance scores and robustness to different responses. In particular, it beat out the other models in the validation study, and was competitive with the top performer in the cross-validation study. Of the other models, the maximin LHS with either kriging or quadratic regression models also showed good performance and robustness to different responses.

The poorest performing design was augmented pairs (AP), which was not competitive with the other three designs. This could be due to the fact that the AP design has fewer runs and is designed to work best with linear modeling approaches like quadratic regression. It does not have the kind of space-filling characteristics that one would expect for good performance using the other types of models. The worst performing modeling approaches were MARS and AVAS, which showed decent performance on some responses, but poor results on others.

1   Introduction

1.1 Background

To understand the behavior of a response function with respect to multiple predictor values, one typically needs a large number of observations to adequately cover the input space. An inefficient approach is to compute the response for all combinations of predictor values chosen on a suitably fine grid. Usually, this is not feasible. In physical experiments, some combinations of predictors may not be available to the experimenter, or may produce responses that are beyond the capability of the instrumentation to measure. In simulated experiments (e.g., finite element computer models), a large amount of computation may be required to collect each response. Therefore, computing responses over a grid of predictor values may take too long, or be too expensive to complete.

The standard method for avoiding costly data collection is to only observe the response at a subset of predictor values, and then fit a metamodel (also called a "proxy model" or "response surface model" or "reduced-order model") to those points. Metamodels approximate the response at unobserved combinations of predictor values using the available sampled data, and are typically designed for rapid prediction. In this way, an approximate response surface can be generated for the entire input space in a short amount of time, and it can subsequently be used to meet project-specific research goals.

1.2 Previous Work

In the oil and gas literature, metamodels are often used as proxies for the underlying simulation models, especially for optimization and uncertainty quantification studies. Osterloh (2008) [1], Ekeoma and Appah (2009) [2], and Zubarev (2009) [3] provide overall guidance on sampling and metamodeling strategy for reservoir simulations. In particular, Osterloh (2008) [1] examines Latin hypercube sampling (LHS) designs and compares polynomial and kriging metamodels, Ekeoma and Appah (2009) [2] focuses specifically on LHS designs, and Zubarev (2009) [3] compares polynomial, kriging, thin plate spline, and artificial neural network metamodels.

There are also examples of specific case studies in which metamodeling was used. Kalla and White (2005) [4] compared a second order polynomial model and kriging model using an orthogonal array (OA) sample design in a gas coning case study. In this case, the second order polynomial outperformed kriging with a 36-run design in 14 variables. Anbar (2010) [5] settled

SIMPLIFIED PREDICTIVE MODELS FOR CO₂ SEQUESTRATION PERFORMANCE ASSESSMENT

RESEARCH TOPICAL REPORT ON TASK #4 REDUCED-ORDER METHOD (ROM) BASED MODELS

Reporting Period: October 1, 2012 through June 30, 2015

Principal Investigator: Dr. Srikanta Mishra
mishras@battelle.org 614-424-5712
Principal Authors: Larry Zhaoyang Jin, Jincong He and Prof. Louis J. Durlofsky
(Author affiliation: Stanford University, Stanford, CA 94305)

Date Report Issued: June 2015

Submitting Organization:

Battelle Memorial Institute
505 King Avenue
Columbus, OH 43201
DUNS Number: 00 790 1598

Abstract

Reduced-order models provide a means for greatly accelerating the detailed simulations that will be required to manage CO_2 storage operations. In this work, we investigate the use of one such method, POD-TPWL, which has previously been shown to be effective in oil reservoir simulation problems. This method combines trajectory piecewise linearization (TPWL), in which the solution to a new (test) problem is represented through a linearization around the solution to a previously-simulated (training) problem, with proper orthogonal decomposition (POD), which enables solution states to be expressed in terms of a relatively small number of parameters. We describe the application of POD-TPWL for CO_2-water systems simulated using a compositional procedure. Stanford's Automatic Differentiation-based General Purpose Research Simulator (AD-GPRS) performs the full-order training simulations and provides the output (derivative matrices and system states) required by the POD-TPWL method. A new POD-TPWL capability introduced in this work is the use of horizontal injection wells that operate under rate (rather than bottom-hole pressure) control. Simulation results are presented for CO_2 injection into a synthetic aquifer and into a simplified model of the Mount Simon formation. Test cases involve the use of time-varying well controls that differ from those used in training runs. Results of reasonable accuracy are consistently achieved for relevant well quantities. Runtime speedups of around a factor of 370 relative to full-order AD-GPRS simulations are achieved, though the preprocessing needed for POD-TPWL model construction corresponds to the computational requirements for about 2.3 full-order simulation runs. A preliminary treatment for POD-TPWL modeling in which test cases differ from training runs in terms of geological parameters (rather than well controls) is also presented. Results in this case involve only small differences between training and test runs, though they do demonstrate that the approach is able to capture basic solution trends. The impact of some of the detailed numerical treatments within the POD-TPWL formulation is considered in an Appendix.

Contents

List of Figures

List of Tables

Executive Summary

The methods and results presented in this topical report represent the accomplishments under Task 4 of the overall project on 'Simplified Predictive Models for CO_2 Sequestration Performance Assessment.' Task 4 was concerned with Reduced-Order Method (ROM) based Models, and the research associated with this task was performed at Stanford University. The need for reduced-order modeling is motivated by the observation that, although flow simulation can be used to design and manage CO_2 sequestration projects, the large number of detailed runs required for some applications (such as computational optimization and uncertainty assessment) can lead to great computational expense. Computationally-efficient procedures, including numerical reduced-order models, which have been applied in related areas such as oil reservoir simulation, may thus be very useful for these problems.

In this work, we explore the use of trajectory piecewise linearization (TPWL) combined with proper orthogonal decomposition (POD) for simulating CO_2 storage problems. POD-TPWL models of this type have been successfully used for oil-water and oil-gas compositional reservoir simulation problems. The basic approach with POD-TPWL is to first perform one (or a few) full-order 'training' runs, which entail high-fidelity (full-order) flow simulations under a prescribed set of well controls (e.g., time-varying bottom-hole pressures or rates). For subsequent (test) runs, which involve different well control settings, the solution at each time step is represented based on a linearization around a training solution. The use of POD, which allows us to represent solution states (e.g., pressure and overall mole fraction in every grid block) in terms of a small number of parameters, along with a constraint reduction procedure, which projects the set of governing equations into a low-dimensional subspace, provides a high degree of efficiency.

The full-order simulations applied in this work use a two-phase, two-component (CO_2 and water) formulation within Stanford's Automatic Differentiation-based General Purpose Research Simulator (AD-GPRS). This simulator was modified to output the state and derivative matrices required to construct the POD-TPWL model. New features introduced in this work, in addition to the application of POD-TPWL to CO_2 sequestration simulations, are the use of rate-control specifications for wells and the incorporation of horizontal injectors into the model. Because of the way in which AD-GPRS represents wells, the use of rate-controlled wells in POD-TPWL requires additional matrix manipulations in the model construction step.

CO_2 storage with both a synthetic (channelized) aquifer and an approximate model of the Mount Simon formation (planned for use with FutureGen 2.0) is considered for test cases that involve wells controlled by both time-varying bottom-hole pressures and rates. Generally accurate results are obtained for well quantities and for CO_2 plume location, though the accuracy of the POD-TPWL model is seen to degrade as the controls used in test cases deviate from those applied in training runs. Runtime speedups with POD-TPWL for these cases are about a factor of 370 relative to high-fidelity AD-GPRS simulations. The overhead required to construct the POD-TPWL model (including training runs) is equivalent to about the time required for 2.3 full-order runs.

The POD-TPWL model is then extended to allow parameters associated with the geologic model to be perturbed in test runs. Preliminary results using this capability in two-dimensional models, in which all block-to-block transmissibilities are multiplied by a constant value relative to the training run, demonstrate that the POD-TPWL model is able to capture general trends in the relevant well quantities. The differences between test- and training-case results are, however, very small in the scenarios considered. Results are also presented for a CO_2-enhanced oil recovery problem, which demonstrates the use of POD-TPWL for problems where CO_2 is both utilized and sequestered.

An Appendix to this report presents a detailed assessment of constraint reduction procedures

for POD-TPWL models of the type considered here. As noted above, the constraint reduction procedure projects the set of governing equations into an appropriate subspace of much lower dimension. The approach used in previous POD-TPWL models of oil-water systems was the Galerkin projection procedure, in which the left-projection matrix is the transpose of the POD basis matrix used to concisely represent the system states. In this work, we show that the use of a (different) so-called Petrov-Galerkin procedure leads to much better stability properties in POD-TPWL models of oil-water and oil-gas compositional systems. This is the approach used in all of the CO_2 storage simulations presented in this report.